



National University of Lesotho



Optimization of Mantsonyane and Semonkong mini hydro power stations by hybridization

BAHLAKOANA DAVID LEPHEANA

A dissertation submitted in partial fulfilment
of the requirements for the degree of

Master of Science in Sustainable Energy

Offered by the

Energy Research Centre
Faculty of Science & Technology

March 2020

Acknowledgements

I would like to acknowledge my supervisor Prof. L.Z Thamae for his great sacrifice, continued support and guidance during the entire process in writing this dissertation. I struggled so much in the beginning but you were so considerate and patient with me until i got back on track. I also acknowledge Dr. Khang who helped me to comprehend some difficult issues with my research and managed to spare time for me in his busy schedule during the most challenging era of my life. In addition, I wish to thank Dr. Chele for clarifying most of the research concepts to me and for her suggestions and advice.

I would like to express my profound gratitude and appreciation to my beloved wife 'Matsireletso, and to my children T'seli and Molemo for their patience and inspiration. I can never thank my wife enough for providing me with unwavering support from the beginning to the end of my research. She patiently performed my role as a father in the family while I was busy with my studies.

Last but not least, greatest thanks go to my employer, Lesotho Electricity and Water Authority (LEWA) for offering me the opportunity to further my studies and most importantly, for financing my studies throughout the duration of the course. I also thank my manager at LEWA, Mr. Monti Ntlopo who opened the opportunity for me to pursue this program as well as his consistent support over the two years of my studies.

Table of Contents

ABSTRACT.....	6
1 CHAPTER 1: INTRODUCTION	8
1.1 Introduction.....	8
1.2 Research Problem	10
1.3 Purpose of the study.....	13
1.4 Significance of the study.....	14
1.5 Research questions.....	14
2 CHAPTER 2: LITERATURE REVIEW	15
2.1 Renewable Energy Resources Assessment	16
2.1.1 Measuring water discharge and head	16
2.2 Determination of river flow variation	16
2.2.1 Measuring wind speed and direction.....	17
2.2.2 Measuring solar radiation.....	18
2.3 Systems components and characteristics	20
2.3.1 Small Hydro Power System	20
2.3.2 Solar PV System.....	26
2.3.3 Wind Power System	29
2.3.4 Weibull Parameters and Speed Frequency Distribution	31
2.3.5 Annual Energy Production (AEP) of a wind turbine	32
2.4 Optimization of Hybrid Renewable Energy Systems.....	34
3 CHAPTER 3: RESEARCH METHODOLOGY	40
3.1 Define the Primary load	43
3.2 Undertake Resource Assessment and describe their properties	44
3.2.1 Solar Resource	44
3.2.2 Hydro Resource.....	45
3.2.3 Wind Resource.....	49
3.2.4 Diesel Fuel	50
3.3 Hybrid system components and Specifications.....	50
3.3.1 Selection of suitable equipment for Semonkong and Mantsonyane	51
4 CHAPTER 4: SIMULATION RESULTS AND DISCUSSIONS	60
4.1 Semonkong Off-Grid Hybrid Power Station.....	60

4.1.1	Simulation Results HRES	60
4.1.2	Optimization Results.....	63
4.1.3	Sensitivity Analysis Results.....	64
4.2	Mantsonyane Grid-Connected Hybrid Power Station.....	66
4.2.1	Simulation Results	66
4.2.2	Optimization Results.....	67
4.2.3	Sensitivity Analysis Results.....	68
5	CHAPTER 5: CONCLUSION AND RECOMMENDATIONS	70

Table of Figures

Figure 1:	Mantsonyane hydropower intake - dry season	10
Figure 2:	Mantsonyane generation during dry season	11
Figure 3:	2017-18 Semonkong energy production from diesel and hydro	11
Figure 4:	2017-18 Semonkong generation hours	12
Figure 5:	2018-19 Semonkong energy production from diesel and hydro	12
Figure 6:	Flow Duration Curve (FDC) [13].....	17
Figure 7:	Cup anemometer.....	18
Figure 8:	Pyranometer - solar radiation measuring instrument.....	19
Figure 9:	Small Hydropower plant main parts.....	21
Figure 10:	Turbine selection chart based on head and flow rate [22].....	22
Figure 11:	(a) Impulse turbine – Pelton wheel (b) Reaction turbine – Francis turbine.....	23
Figure 12:	Typical efficiency curves for different types of hydropower turbines [22].....	25
Figure 13 (a):	A solar cell	26
Figure 13 (b):	A solar module	
Figure 14:	PV module construction	26
Figure 15:	Modules connected in series to form a string	27
Figure 16:	Modules connected in parallel.....	27
Figure 17:	Strings connected in parallel	27
Figure 18:	Solar cell I-V Characteristic Curve [27].....	28
Figure 19 (a):	Horizontal axis wind turbine	29
Figure 19 (b):	Vertical axis wind turbine.....	
Figure 20:	Wind Turbine Power Output Curve [31].....	31
Figure 21:	Weibull probability density curves for a range of values of k [32].....	32
Figure 22 (a):	Wind turbine Power curve	33
Figure 22 (b):	Probability Density Function (PDF).....	
Figure 23:	Wind Turbine Generator Components [35].....	34
Figure 24:	Benin's electricity supply (2005–2015): national production vs. import [36].....	35
Figure 25:	Lesotho Electrical Energy purchases and sales [5]	36
Figure 26:	Proposed system configuration.....	40
Figure 27:	Methodology block diagram.....	41
Figure 28:	Semonkong daily load profile	43
Figure 29:	Mantsonyane’s simulated minimum daily load profile	44
Figure 30:	Semonkong and Mantsonyane’s daily radiation and clearness index	45

Figure 31: Average monthly streamflow for Mantsonyane River	45
Figure 32: Average monthly streamflow for Maletsunyane River	46
Figure 33: Monthly Average streamflow for Maletsunyane River (15 years).....	47
Figure 34: Monthly Average streamflow for Mantsonyane River (12 years).....	47
Figure 35: Maletsunyane River FDC and Power curve	48
Figure 36: Mantsonyane River FDC and Power curve	49
Figure 37: Average wind speed at Semonkong and Mantsonyane	50
Figure 38: (a) Semonkong Hybrid system modelling (b):Mantsonyane Hybrid system modelling	51
Figure 39: Solar PV module (Semonkong).....	52
Figure 40: Solar PV module (Mantsonyane)	52
Figure 41: Power curve and annual yield of XANT M-21 wind turbine model [52].....	53
Figure 42: Semonkong and Mantsonyane’s wind speed PDF	53
Figure 43: Wind turbine generator (Mantsonyane).....	54
Figure 44: Wind turbine generator (Semonkong)	54
Figure 45: Storage battery (Semonkong)	54
Figure 46: Storage battery (Mantsonyane).....	55
Figure 47: Semonkong hydro power station – Sinexcel 500 Converter	55
Figure 48: Semonkong hydro power station – 180 kW Francis turbine	56
Figure 49: Semonkong hydro power station - SCANIA DA3-AJ550P-5S1diesel generator	56
Figure 50: Mantsonyane hydro power station – 2 MW Francis turbine	57
Figure 51: Mantsonyane hydro power station – Eaton Xpert 2250 kW.....	57
Figure 52: Semonkong hybrid power system simulation results (LCOE optimized)	61
Figure 53:Electricity generation and consumption (LCOE optimized) – Semonkong	62
Figure 54: Semonkong hybrid power system simulation results (RF optimized).....	62
Figure 55: Electricity generation and consumption (RF optimized) – Semonkong.....	62
Figure 56: Fuel summary for Semonkong HRES	64
Figure 57 : Effects of fuel price and load variation on the COE and O&M cost – Semonkong HRES.....	65
Figure 58: Effect of river flow rate and discount rate on the COE and NPC – Semonkong HRES	65
Figure 59: Mantsonyane hybrid power system simulation results (LCOE optimized).....	66
Figure 60: Electricity generation and consumption (LCOE optimized) – Mantsonyane.....	66
Figure 61: Mantsonyane hybrid power system simulation results (RF optimized)	67
Figure 62: Electricity generation and consumption (RF optimized) – Mantsonyane	67
Figure 63: Effects of solar radiation and flow rate on capacity shortage and COE – Mantsonyane HRES68	
Figure 64: Effects of solar radiation and wind speed on COE and Annual Energy Production – Mantsonyane HRES.....	69

List of Tables

Table 1: Technical Specification of Components	58
--	----

ABSTRACT

This paper shows the optimized design and performance of a hybrid energy system for the following study sites, Mantsonyane and Semonkong in Lesotho. The main objective is to design a hybrid system with Low Cost of Energy (LCOE), high Renewable Fraction (RF) and reduced carbon emissions from a diesel generator at Semonkong hydro-diesel hybrid system. This study employs HOMER Pro simulation software to demonstrate the performance of the Mantsonyane and Semonkong hybrid renewable energy systems.

The proposed Semonkong system design is made up of 360 kW of solar PV array, 100 kW wind turbine, 500 kW inverter, 1 MWh battery storage, 180 kW mini hydro and 410 kW diesel generator with a Load Following (LF) dispatch strategy. The simulation results indicate the environmentally friendly system with a renewable fraction of 97.3% which also reflects the high utilization of renewable energy in the system and the remaining small portion is diesel generator. The total energy produced is 1,978,099 kWh per year out of which 25.2% is contributed by wind turbines, hydro power generation contributed 41.8% while solar PV supplied 31.6% and diesel generator injected only 1.42%.

The LCOE for this system is \$0.129/kWh and these results are taken at the solar irradiation of 5.44 kWh/m², wind speed of 9.71 m/s, average flow rate of 1,595 L/s and the diesel price of \$1.00/L. The project would demand an initial capital contribution of roughly \$1.25M with a total NPC of \$2.65M. The proposed Mantsonyane system design comprises of twenty-five wind turbines with a total capacity of 7.5 MW, one unit of 1MWh battery storage, 2 MW mini hydro turbine and a 2 MW converter. The simulation results show that the renewable fraction for the most cost effective system configuration is 100% with the LCOE of \$0.149/kWh. The results were taken at the solar irradiation of 5.44 kWh/m², wind speed of 9.71 m/s, and average flow rate of 1,731 L/s. This project would demand an initial capital contribution of roughly \$22.8M with a total NPC of \$45.2M.

Sensitivity analysis is used to investigate the impact of variation in wind speed, solar radiation and river flow rates at Mantsonyane. The analysis indicates that a high COE is experienced when the plant is operating at a very low load with comparatively low O&M costs. It is also found that good river flow rates and high wind speeds result in a more affordable unit price. As for Semonkong site, the optimal solution shows a minimal impact from the instability of diesel price, river flow

rate and solar radiation. The LCOE drops with the increasing wind speed and river flow rates. However, the diesel generator will remain part of the system in order to boost generation during dry season from July to September.

1 CHAPTER 1: INTRODUCTION

1.1 Introduction

The continuous depletion of fossil fuels and the effects brought about by the global climate change have directed the international research focus towards the development of Renewable Energy Sources (RESs). High interest is on the most available RESs like hydro, wind and solar energy. On the other hand, wind and solar energy are highly intermittent and unpredictable while hydro energy is mostly affected by the changing patterns of rainfall as a result of climate change. In order to mitigate against the intermittency of wind and solar resources, multi energy integrated systems play a critical role in making use of diverse RESs. Coupling two or more types of energy sources leverage complementarity to achieve stable and quality power output [1].

Similarly, the main purpose of developing Hybrid Renewable Energy Systems (HRES) is to use the strengths and advantages of one source to counterbalance those of the other source, this means that the energy sources can complement each other in this manner and at least one of the sources would be available for power generation when others are not. For instance, at night when the sun is not there, the system can rely on hydro and or wind resource. HRES is simply an electrical system that combines at least two different energy sources with at least one of them being a renewable energy source. The main purpose of HRES is to meet the load demand from RES, and in case of shortage of supply, the conventional sources fill the gap while minimizing the fuel consumption [2].

According to Kartite and Cherkaoui , hybrid renewable energy systems can be classified into two categories, namely [2]:

- **Grid connected hybrid system;** this system is physically connected to the grid and operates in parallel with the electrical network.
- **Stand-alone hybrid system;** this system is isolated from the grid and operates on island mode.

The hybrid system can further be categorized into three types of systems:

- **A system with or without a conventional energy source;** A hybrid system can have a conventional power source such as a gas turbine, a diesel generator or the whole hybrid plant connected to the grid.
- **A system with or without storage;** A storage device is highly imperative for autonomous hybrid systems. The storage feeds the load if there is insufficient RE source to supply the load. Rechargeable batteries are a commonly used type of storage.
- **A renewable energy source used;** A HRES should consist of a renewable energy source, either wind or solar PV or hydro or even a combination of these sources. The choice of the source is determined by the available energy potential.

This study is going to assess the viability of developing a grid and off-grid Hybrid Renewable Energy Systems (HRES) for Mantsonyane and Semonkong mini hydropower plants respectively. This study will also cover the evaluation of the potential of renewable energy sources available at these two areas as well as the possibility of exploiting their related technologies. The study area at Mantsonyane is geographically located at S 29° 35' 44"; E 28° 17' 40", 2215 m above sea level while the Semonkong study area is geographically located at S 29° 49' 22" ; E 28° 1' 39", 2192 m above sea level. Mantsonyane power station is a run-off-river mini hydropower plant with a small rock fill intake and its generation is mainly driven by the availability of water. It is grid connected with 35 m head and a capacity of 2 MW made up of two units, one unit is rated at 1500 kW and the other at 500 kW. A horizontal Francis turbine is used for the Mantsonyane plant.

Semonkong power station is an off grid run-off-river mini hydropower plant with a 180 kW, horizontal Francis turbine with a rated head of 18 m, and a 400 kW diesel generator to form a net capacity of 580 kW. Due to the absence of enough water storage, the hydro part of the plant does not generate enough power especially in dry but cold winter seasons. The load at such times is fed entirely from a diesel generator and this becomes too costly and not environmentally friendly. As a result of the high diesel cost, the Semonkong generation is currently scheduled to supply load from 07:00 to 22:30 in the evening.

1.2 Research Problem

Considering the current situation in the sub-Saharan Africa regarding sustainability of hydropower generation, it can be seen that the energy production from hydropower plants is deteriorating at an alarming rate [3]. If this condition continues for extended periods without proper mitigation strategies in place, the region would be in economic crises. Research has shown that by 2050, annual water discharge in the Zambezi basin is likely to drop by 20% and this declining trend in discharge is predicted to worsen with time [4]. It is expected to reach about 40% to 50% by the end of the 21st century and this would definitely pose a great risk for water resources management in the Zambezi basin.

The current situation in Lesotho is that the country is frequently experiencing severe droughts and this results in loss of generation from the Mantsonyane and Semonkong hydropower stations. In addition, Lesotho has been experiencing about 1.5% steady increase of capacity deficit since 2013, this trend continued in that manner because the national demand increases every year with a fixed installed capacity of 74.7 MW [5]. With reference to Figure 1, it can be observed that during the dry season the Mantsonyane mini hydro power intake goes completely dry. In addition to this, there is a challenge of sedimentation which reduces the capacity of the pond and as a result the plant is not generating at all as illustrated in Figure 2. In order to meet the national demand, the local generation has to be supplemented by additional power imported from South Africa and Mozambique at a significant cost to the country.



Figure 1: Mantsonyane hydropower intake - dry season

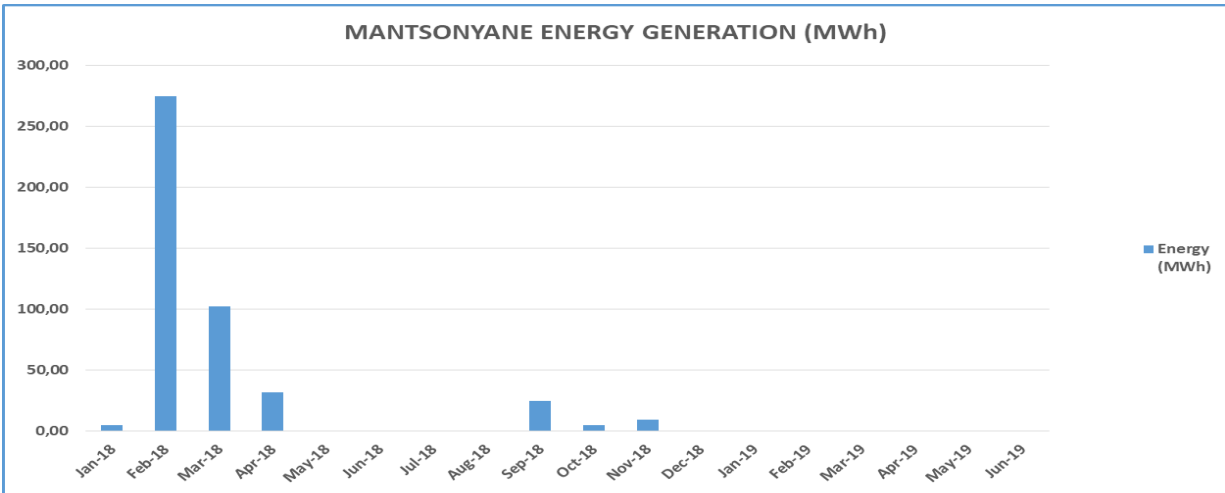


Figure 2: Mantsonyane generation during dry season

The main focus of this study in relation to the Mantsonyane mini hydro is to maintain or go above the intended generation power of 2 MW to be fed to the grid throughout the year with the introduction of other renewable energy sources. In addition to the renewable energy sources, the battery storage was considered in order to ensure availability of supply during the absence of any of the renewable energy sources. The grid in this case is therefore regarded as the load.

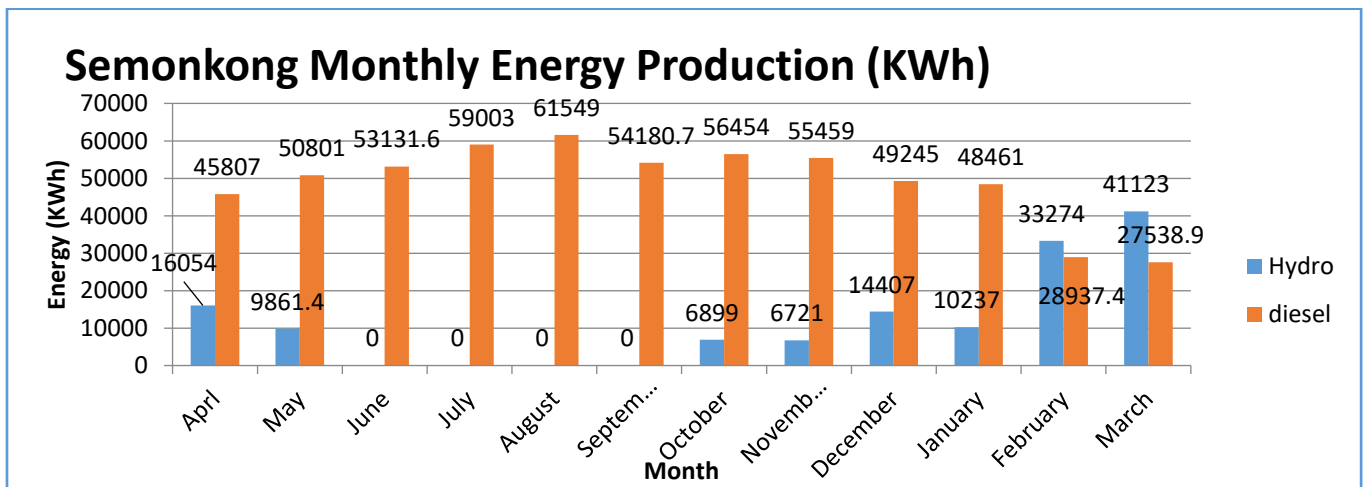


Figure 3: 2017-18 Semonkong energy production from diesel and hydro

It can be observed from Figure 3 that during 2017-18 the energy production was mainly from diesel generator. Hydro energy production started to decline from April until it reached zero in

June, the hydropower plant remained off until September 2017 and started to generate from October up to March 2018. During this period, Semonkong total annual generation time was 5,939.95 hours, of which 1,485.45 hours is hydro and 4,454.5 hours is contributed by diesel as depicted in Figure 4, this translates to 68 % of the total number of hours in a year. In the same period, the total energy produced was 743,203.1 kWh, of which only 139, 051.4 kWh is from hydro and 604, 151.7 kWh is from diesel generator. Following from the above, the intention of this study with regard to Semonkong is to ensure that the plant production meets the load and operates all the time. The following Figure 4 and Figure 5 show the monthly generating hours and monthly energy production respectively.

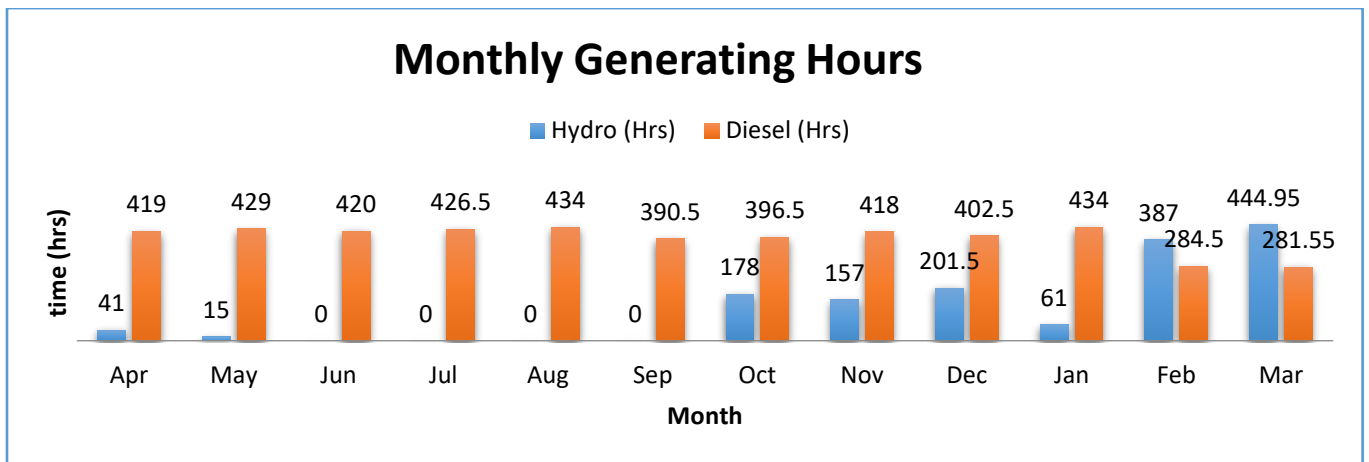


Figure 4: 2017-18 Semonkong generation hours

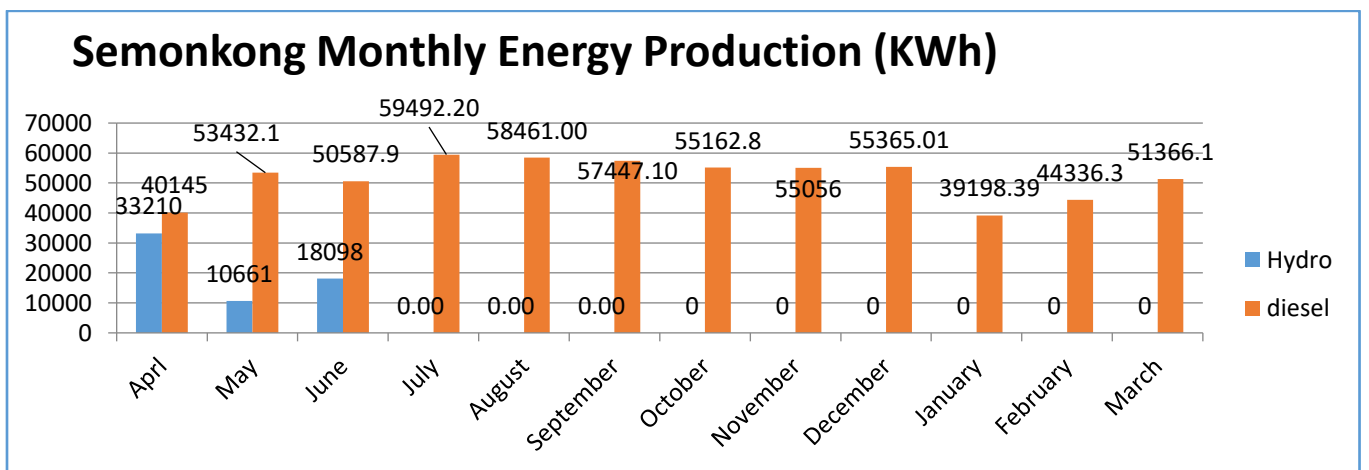


Figure 5: 2018-19 Semonkong energy production from diesel and hydro

However, much of the energy production was from diesel generator during 2018-19 and the production further declined during this period as illustrated in Figure 5. Hydropower plant only produced energy for three months from April 2018. Semonkong relied on diesel generator from July 2018 to March 2019. The total energy generated during this period was 682, 018.9 kWh, of which 61,969 kWh was from hydro and diesel generator contributed 620, 049.9 kWh. During the same period, Semonkong total annual generation time was 5,743.5 hours, of which 1,485.45 hours is hydro and 4,454.5 hours is contributed by diesel. This translates to 65 % of the total number of hours in a year.

1.3 Purpose of the study

The purpose of the study is to examine the viability of incorporating solar PV, wind and battery storage power systems into the existing unreliable Semonkong hydro-diesel generator and a grid connected Mantsonyane hydro system. The study aims at investigating the ways in which the diesel consumption and the diesel generator operating hours can be reduced at Semonkong hydro – diesel hybrid in order to provide a reliable, cost effective and environmentally friendly energy supply. This research aims at investigating the most cost-effective system configurations in terms of the minimum LCOE. The study will first assess the potential of wind and solar resources and offer recommendations on renewable energy sources that have a potential to generate power at each of the study sites. The research will focus on establishing the most cost effective and optimal configurations of the HRES for the Mantsonyane grid-connected hydropower system and the Semonkong off-grid hydropower-diesel system.

A proper selection and sizing of components for HRES would be achieved by the use of Hybrid Optimization Model for Electric Renewables (HOMER) software to simulate the system for optimization and sensitivity analysis. HOMER allows users to input technical and financial parameters for simulation of the operations of mini grid designs. More importantly, HOMER is capable of optimizing system configuration and offers a list of feasible schemes ranked on the bases of Net Present Cost (NPC) and Levelised Cost of Energy (LCOE). It does hundreds of hourly simulations with the purpose of making sure that the best combination to match demand and supply is identified [6].

1.4 Significance of the study

The existing renewable energy projects in Lesotho are based on stand-alone solar PV, grid tie solar PV without storage as well as hydro power plants without integration of other renewable energy sources. According to Falchetta et al, in most cases the mix of wind, solar PV and hydro would be comparatively less costly than the single renewable energy source plant [7]. In addition to that, the renewable energy generation mix normally comes with the advantage of access to clean and affordable energy. If other renewable energy sources are included, the environmental pollution caused by burning of fossil fuels to produce power at Semonkong would also reduce and that would create a clean environment for the community in that area. Equally important is that the operational costs incurred by the system operator (Lesotho Electricity Company) will be reduced. It is also anticipated that there will be a remarkable increase of energy supplied to the grid if wind and solar PV would be integrated into the Mantsonyane mini hydropower station. This will consequently cut down the import bulk energy purchases and benefit the system operator as it will realize a saving on energy purchasing.

1.5 Research questions

The following questions will be answered by this study:

- How viable it is to develop a grid connected Hybrid Renewable Energy System at Mantsonyane that is comprising hydro, wind, battery storage and solar resources?
- How viable it is to develop an off-grid hybrid energy system at Semonkong that is comprising of diesel generator, hydro, wind, battery storage and solar resources?
- What would be the most cost-effective system configurations in terms of the minimum LCOE?

This report is structured into five chapters. Chapter one covers the introduction of the topic while chapter two presents a review of the literature on hybrid energy systems. In chapter three, a step by step methodology adopted to complete the project is highlighted as well as the characteristics and specifications of the number of components for the proposed hybrid systems. The results of this study and the discussions are presented in chapter four. Lastly, chapter five provides the conclusions and recommendations.

2 CHAPTER 2: LITERATURE REVIEW

It is quite evident that the fossil fuel resources are diminishing at an alarming rate due to high energy demand in different sectors. In response to this crisis, alternative energy resources like hydro, biomass, wind, solar, and geothermal are being used in most areas around the globe lately. While this is the case, since renewable resources like wind and solar are comparatively intermittent, their Plant Capacity Factor (PCF) is significantly lower compared to conventional generating plants [8]. PCF is defined as the ratio of the plant energy production over a certain period of time to the energy that would have been produced if the plant had operated continuously at its rated capacity. Therefore the annual PCF is given by equation (1) [9] as:

$$PCF (\%) = \frac{\text{Energy generated per year (kWh/year)}}{\text{Installed capacity (kWh)} * 8760 \text{ hours/year}} \quad (1)$$

Plant capacity factor illustrates the extent of the utilization of the generating plant. This means that the plant which operates continuously at its rated capacity has the capacity factor of 100% or unity. Research has revealed that a hybrid renewable energy system offers a better option than a single source system in terms of reliability, efficiency and cost effectiveness. For this reason, more than one energy sources are being used in hybrid renewable energy system as stand-alone or in grid tie mode [10]. It is feasible to have different types of hybrid system combinations depending on the availability of resources at the study area. Studies have shown that the choice of different configurations and combinations of RE sources is determined by the climate characteristics of the area of project implementation. This is highlighted in the following examples [2];

- A combination of a conventional source and wind systems is normally implemented in windy areas such as islands. When this type of a hybrid system operates in stand-alone mode, a storage is a requirement.
- A combination of PV-wind-diesel is widely used where there is a high solar potential and considerable wind speed.
- Hybrid systems without conventional energy sources are normally operated in standalone mode in remote areas where grid extension or supply of fuel is difficult and costly.

- A PV-wind-hydro-storage hybrid system is used where high level of reliability is required, and where a continuous supply is required. This combination, compared to other systems discussed earlier, has a relatively lower price per kilowatt-hour produced.

2.1 Renewable Energy Resources Assessment

2.1.1 Measuring water discharge and head

Discharge is defined as the amount of water passing a specific point over a set time period and is expressed as cubic meters per second (m³/s). Head is the vertical distance that water drops as a result of gravity. Discharge can be measured by different methods such as the area and speed method as well as the bucket method. When measuring flow rate in low flow streams, the bucket method is preferable. In this method, the time taken to fill a bucket is recorded and the flow rate is calculated by dividing the volume of water in the bucket with the time taken to fill the bucket. On the other hand, to measure the flow rate for higher flow streams, the area and speed method is used. With this method, the cross-sectional area is calculated as the product of width and average depth of the river. The discharge is then found by multiplying cross sectional area with water speed flow [9]. The discharge can be calculated by Equation (2) as:

$$Q = V_{avg} \cdot S \quad (2)$$

2.2 Determination of river flow variation

There are mainly two ways in which the variation in river flow can be expressed, the annual hydrograph and the Flow Duration Curve (FDC). The annual hydrograph simply indicates a daily variation flow over a calendar year while FDC is more preferred because it can be used for calculating the energy available at a selected site. FDC indicates the distribution of flow over a certain period, normally a year [11]. With reference to Figure 6, it can be noted that the vertical axis represents the flow rate while the horizontal axis gives the percentage of the time in a year that the stream flow equals or exceeds the corresponding value on the vertical axis. To give an example, a 70% exceedance gives a flow rate of 1m³/s, this says the flow is equaled or exceeded for 70% of the time. In the same way, the FDC can immediately show the flow level that can be

available for at least 50% of the year and is denoted by (Q_{50}). On the other hand, the minimum river flow is taken as the flow that is exceeded for 95% of the year and is taken as (Q_{95}). In line with this theory, a heavy flow river is characterized by a flatter FDC and this means that the average flow is spread almost evenly over the year and this flow pattern gives a useful flow for a longer period [12].

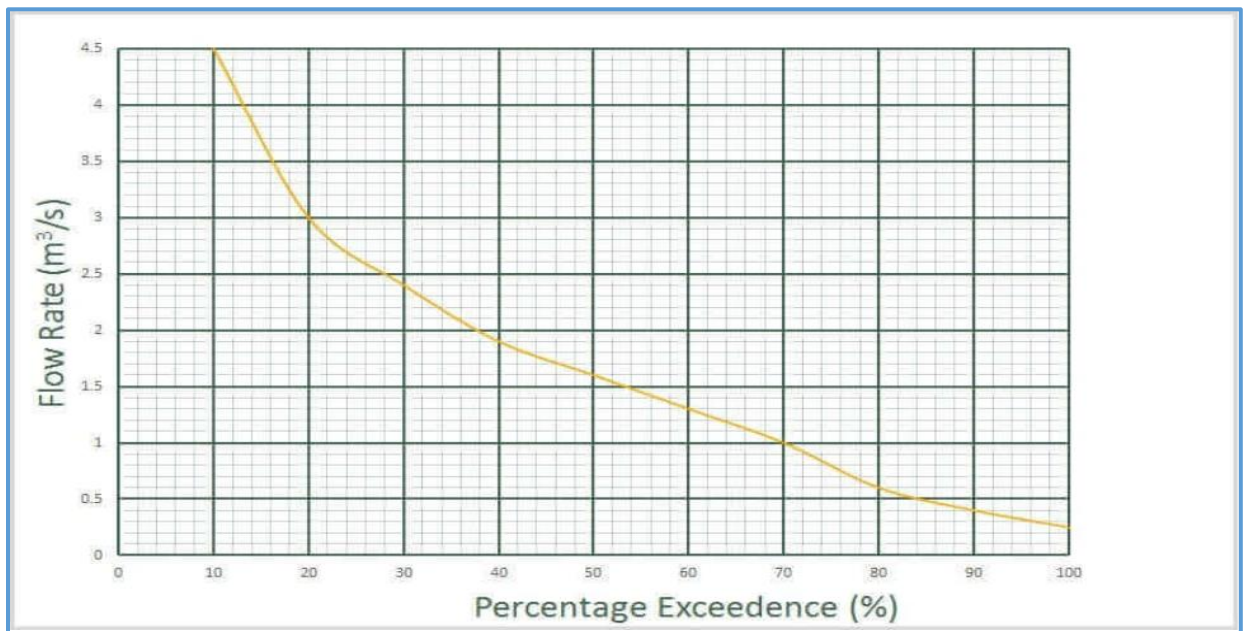


Figure 6: Flow Duration Curve (FDC) [13]

2.2.1 Measuring wind speed and direction

Wind resource assessment is the process of establishing how much energy will be produced from a wind power plant over the course of its useful life. Wind resource characteristics include wind direction, air density and horizontal wind speed. Air density depends mainly on temperature and elevation, it determines the amount of energy available in the wind at a certain speed, and this means more electric power can be obtained at a greater air density [14]. The cup anemometer is used to measure horizontal wind speed. This instrument consists of three or four cups attached to a vertical shaft as depicted in Figure 7, the wind causes the cup assembly to rotate. The internal transducer changes the rotational speed into current which is sent to the data logger. The data logger translates that electrical signal to a wind speed. However, if the measurements for wind speed were not taken at the reference height, there is a possibility to extrapolate the wind speeds to the preferred wind turbine hub height as in equation (3).

$$V(z) \ln\left(\frac{Z_r}{Z_o}\right) = V(Z_r) \ln\left(\frac{Z}{Z_o}\right) \quad (3)$$

where Z_r is the reference height (m), Z is the hub height (m) where the wind speed is to be found, Z_o is the surface roughness, $V(z)$ is the wind speed (m/s) at height z (m) and $V(Z_r)$ is the wind speed at the reference height (m/s).



Figure 7: Cup anemometer

2.2.2 Measuring solar radiation

To determine the availability of solar radiation at any location on earth, there is a number of important parameters to be measured. These include global radiation, sunshine hours, diffuse radiation, beam radiation, temperature, air mass, humidity, wind speed and visibility. Radiation energy at a particular area can be assessed by performing a solar radiation measurement at the site or by making use of a solar radiation model [15]. First of all, a Geographical Information System (GIS) analysis has to be performed to determine the most promising sites. This exercise excludes

settlements and areas with steep slopes, the rest of the area is then categorized using maps of the long term yearly Direct Normal Irradiance (DNI). Then the yearly and monthly mean DNIs and their deviations can be established by using a long term data set of the minimum of 10 years [16].

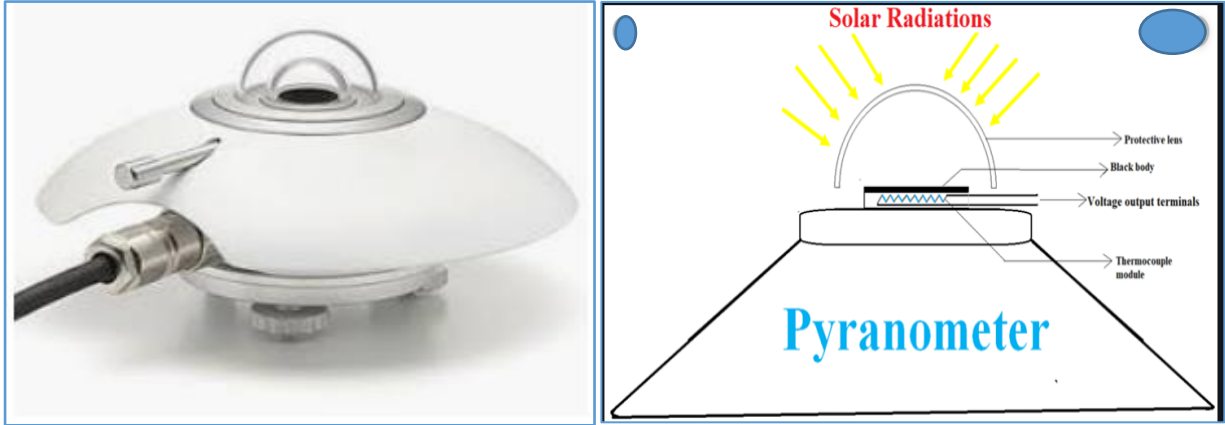


Figure 8: Pyranometer - solar radiation measuring instrument

While this is the case, the measurement of direct and diffused radiation can be done in two primary ways. These values are measured with the use of either ground based instrumentation like pyranometers as shown in Figure 8 or remotely using satellites. It is recommended that both methods be used together in order to validate data [17]. A pyranometer consists of a thin black surface supported inside a polished case. As solar radiation hits this shiny surface, its temperature rises and this results in a small electro-motive force (e.m.f) generated and measured by a millivoltmeter. In the absence of a properly recorded solar radiation data, it is possible to calculate the monthly average solar radiation using equation (4) [15].

$$H = H_o \left(a + b \left(\frac{S}{S_o} \right) \right) \quad (4)$$

where H is the monthly average daily solar radiation on a horizontal surface (kW/m^2), H_o is the monthly average daily extraterrestrial solar radiation on a horizontal surface (kW/m^2), S is the monthly average daily number of clear sunshine hours, and S_o is the maximum possible daily hours of clear sunshine. Coefficient a and b are regression coefficients.

The monthly average extraterrestrial radiation is calculated using equation (5) [18] as:

$$H_o = \frac{24 * 3600 * G_{SC}}{\pi} \left(1 + 0.033 * \cos\left(\frac{360n_d}{365}\right) \right) * \left(\cos\phi \cos\delta \sin\omega_s + \left(\frac{\pi\omega_s}{180}\right) \sin\phi \sin\delta \right) \quad (5)$$

where n_d is the day number starting from the first day of January as 1, G_{SC} is the solar constant (1367 W/m²), ϕ is the location latitude, δ is the declination angle in degrees and is given by equation (6), and ω_s is the sunset hour angle in degrees and is given by equation (7). The maximum possible sunshine hours S_o is calculated using equation (8) [18].

$$\delta = 23.45 \sin\left(360\left(\frac{284 + n_d}{365}\right)\right) \quad (6)$$

$$\omega_s = \cos^{-1}(-\tan\phi \tan\delta) \quad (7)$$

$$S_o = \frac{2}{15} \cos^{-1}(-\tan\phi \tan\delta) \quad (8)$$

2.3 Systems components and characteristics

2.3.1 Small Hydro Power System

Small Hydro Power (SHP) Systems are grouped according to the installed capacity. The systems are further categorized into pico whereby most of the institutions classify pico under the system with a capacity of 10 kW or less, mini is considered as a system with a capacity more than 100 kW but less than 1 MW while small hydro is taken to be any system bigger than 1 MW but smaller than 10 MW [19]. A typical small hydropower system is comprising the basic components as shown in Figure 9. Usually, a run-of-river system has a small or no storage facility, it mainly provides power for the base load with a small flexibility of operation for frequent fluctuations in demand by regulating the water flow to the turbines [20]. This is achieved by running water which is diverted from a flowing river and guided through a penstock which is attached to the turbines in the generator house. The force of the running water spins the turbine and since the turbine is mechanically connected to the generator, the turbine drives the generator and the electricity is produced.

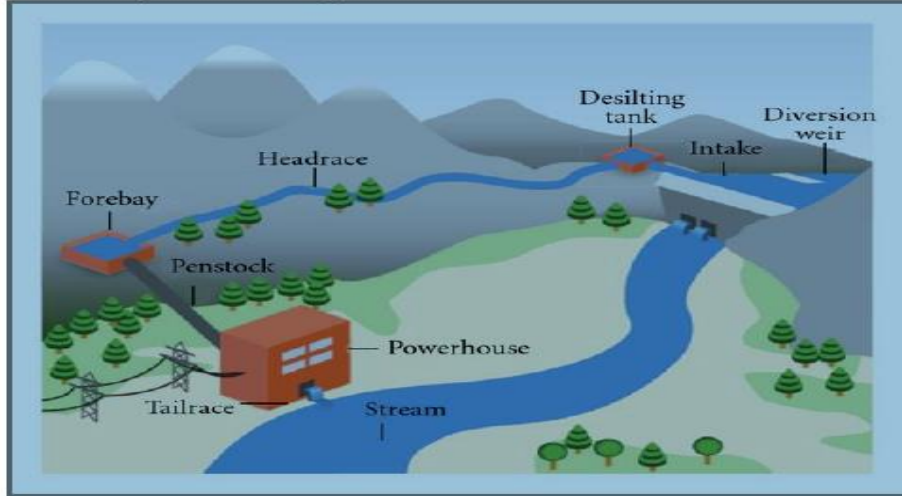


Figure 9: Small Hydropower plant main parts

A hydropower system is normally installed in a location that has adequate stream water throughout the year [7]. The electrical power generated by a hydro power generator is given by Equation (9) as:

$$P = \eta \cdot \rho \cdot g \cdot h_n \cdot Q \quad (9)$$

where P = Power in watts (W), η = Overall efficiency of hydro system ($0 < \eta < 1$), ρ = Fluid density [kg/m^3] (approx. $1000 \text{ kg}/\text{m}^3$ for water), g = Gravitational acceleration ($9.81 \text{ m}/\text{s}^2$), h_n = Net Head in (m) and Q = Volume flow rate (m^3/s) = $\text{Vol}/\Delta t$.

The net head (h_n) can be calculated by subtracting the penstock stock losses and valve losses from the gross head (h_g) as illustrated in equation (10).

$$h_n = h_g - h_f \quad (10)$$

where h_n = Net head (m), h_g = Gross head (m), h_f = Head loss due to friction (m)

While the total energy delivered (E) in kWh is given by Equation (11) as:

$$E = P \cdot t \quad (11)$$

where P = Power (kW) and t = Time (hours)

With reference to Equation (9), it can be observed that in order to make the flowing water turn the turbines, there has to be a head or height from which water flows down to the turbines. The kinetic energy of the water will be transformed into mechanical energy by a hydraulic turbine and finally be converted to electrical energy by generators [21]. As a matter of fact, the conversion of energy from one form to the other results in a loss of energy through the whole system. The turbine is not 100% efficient when it converts energy of falling water into motion energy to spin the generator. The generator is also not 100% efficient at transforming turbine motion into energy and therefore the overall efficiency of the hydropower system in Equation (9) becomes:

$$\eta = \eta_T \cdot \eta_G \quad (12)$$

where η_T = Efficiency of a turbine ($0 < \eta < 1$) and η_G = Efficiency of a generator ($0 < \eta < 1$).

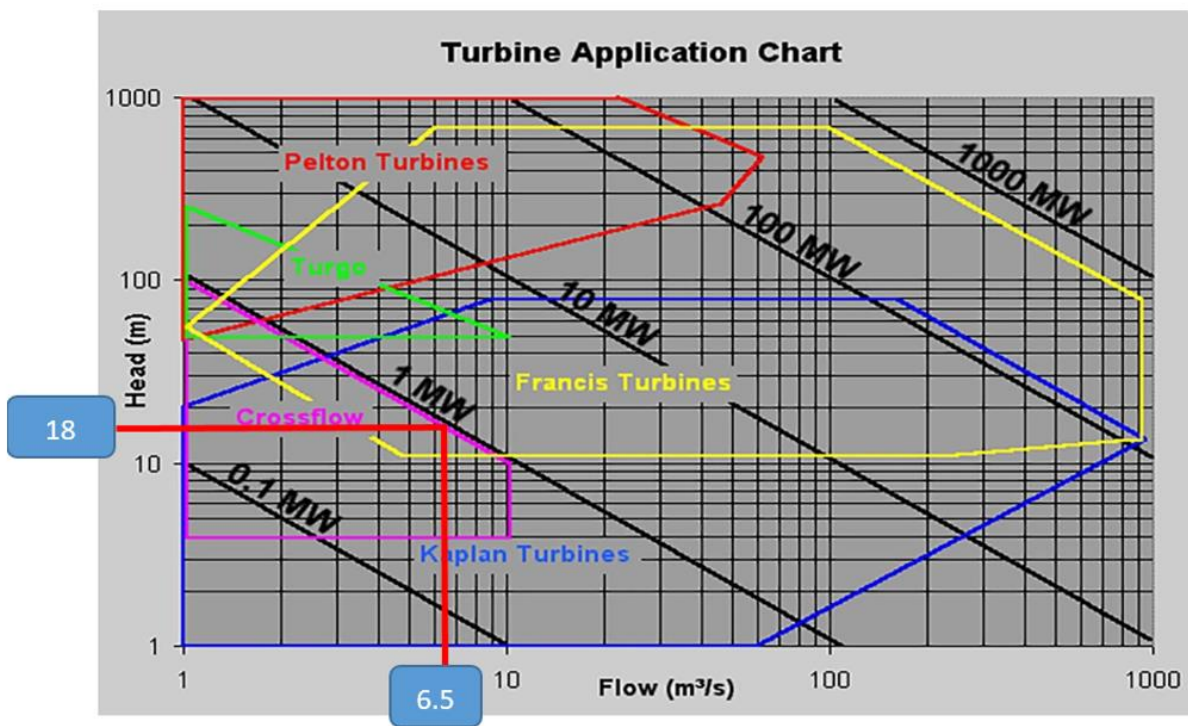


Figure 10: Turbine selection chart based on head and flow rate [22]

One of the critical tasks in the operation of the hydropower system is the choice of an optimum turbine type. Turbines can be selected to suit the available head and flow conditions at the project

site and this can be done with the help of Figure 10 [9]. It can be seen from this chart that Kaplan and Francis turbines can be reliably used in low and medium head sites with power needs of more than 1 kW. Crossflow turbines can be suitable for head ranges from 2m up to 100m with power requirements of 5 kW up to 200 kW, while Pelton turbines can be effectively and specifically utilized for high head sites with estimated power of 50 kW and more [22]. As an example, if 180 kW of electrical power is required for a site with a discharge of 6.5 m³/s with 18 m head then a Francis turbine would be chosen as shown in Figure 10. Relative efficiency is one of the key factors that indicate how suitable a turbine is for a specific site, different hydraulic turbines have their characteristic efficiency over a range of head and discharge as illustrated in Figure 13. It can be seen that the efficiency for propeller and Crossflow turbines improves with the increase in head. These type of turbines are suitable for sites with variable head [23]

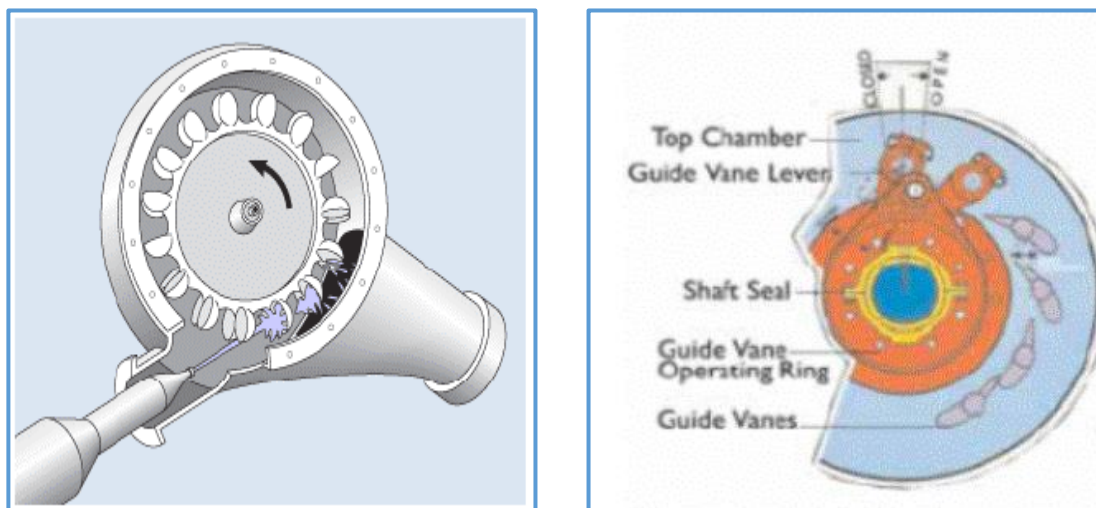


Figure 11: (a) Impulse turbine – Pelton wheel (b) Reaction turbine – Francis turbine

Hydraulic turbines have two main types being reaction and impulse turbines as illustrated in Figure 11.

- A. **Impulse Turbines:** With reference to Figure 11 it can be seen that impulse turbines have a wheel with cups around it. As pressurized water from the penstock is converted to high speed water jets, it hits the turbine cups to cause rotation as illustrated in Figure 11 (a). Pelton wheel, Turgor wheel and gross flow turbines are examples of impulse turbines. They are designed to operate with medium or high head above 10m.

B. Reaction Turbines: Reaction turbines are designed to function under pressure, this turbine has a stator in the form of spiral casings or guide vanes. As the water passes through the guide vanes, it is forced to twist and the angular momentum of the water forces the wheel to rotate as illustrated in Figure 11 (b). Examples of reaction turbines are Kaplan and Francis, they are normally used for low head less than 10m, however they can also perform well in the low head less than 5m [24].

Hydraulic turbines are also selected based on specific speed of a turbine. Specific speed relates the power output of the turbine to its rotational speed and the net head. This is the speed at which an ideal pump similar to the actual pump would develop a one kilowatt power under one meter head as given in equation (13) [25].

$$N_s = \frac{NP^{0.5}}{H^{\left(\frac{5}{4}\right)}} \quad (13)$$

where N = turbine speed (rev/min), P = shaft power (kW) and H = net head (m)

In addition to this, different types of hydraulic turbines have different efficiencies in relation to discharge, this is illustrated in Figure 12. The relationship between discharge and efficiency is given by equation (14).

$$\eta = \eta_R \left(\frac{Q}{Q_R} \right)^{0.5} \quad (14)$$

where η is instantaneous efficiency of a turbine, η_R is the turbine rated efficiency, Q is the instantaneous discharge (m^3/s), Q_R is the turbine rated discharge (m^3/s). It can be seen that the reduction in stream discharge (Q) caused the efficiency (η) to reduce disproportionately.

With reference to Figure 12, it can be observed that the performance of the propeller turbines is more susceptible to flow fluctuations than Francis, Pelton, Kaplan and crossflow turbines. Pelton turbine is the most efficient turbine with the optimum efficiency of about 90% [26]. This turbine can even maintain an optimum efficiency for a wider range of discharge values. Crossflow turbine

efficiency is comparatively lower at around 80% and it can sustain optimum efficiency for a variable span of discharge values.

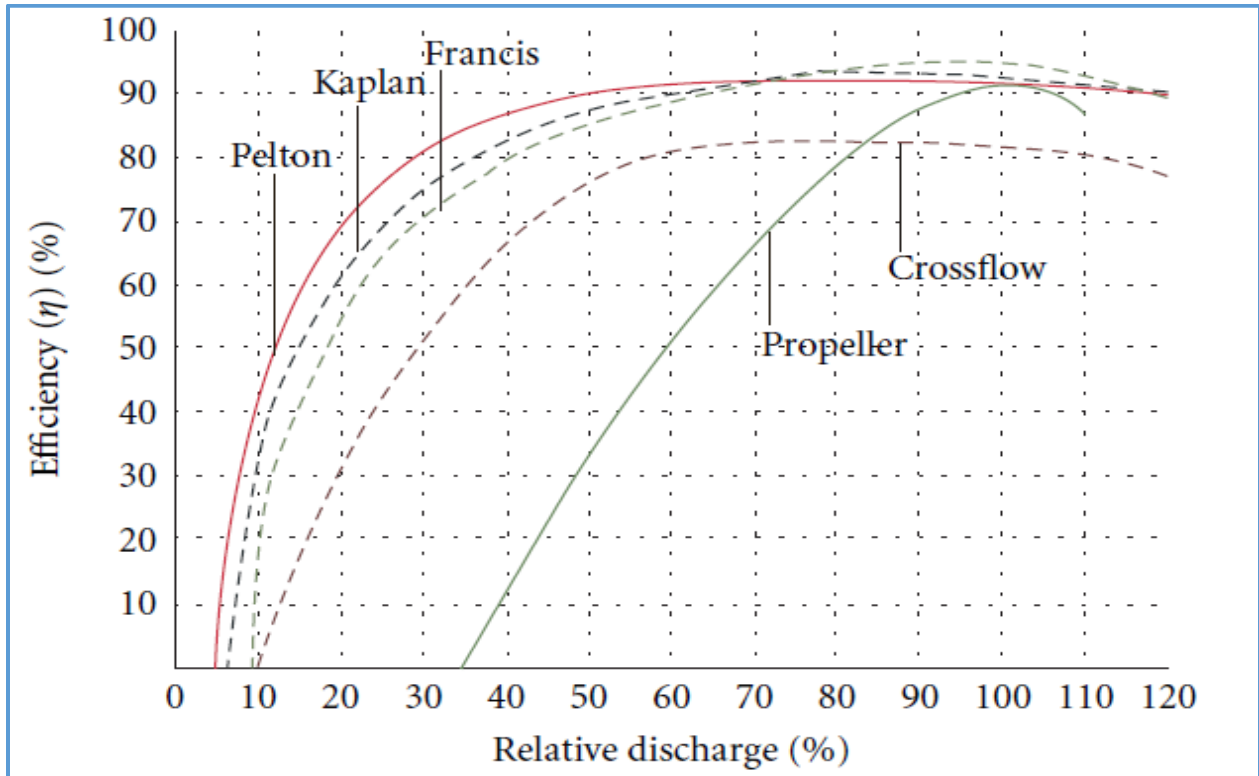


Figure 12: Typical efficiency curves for different types of hydropower turbines [22]

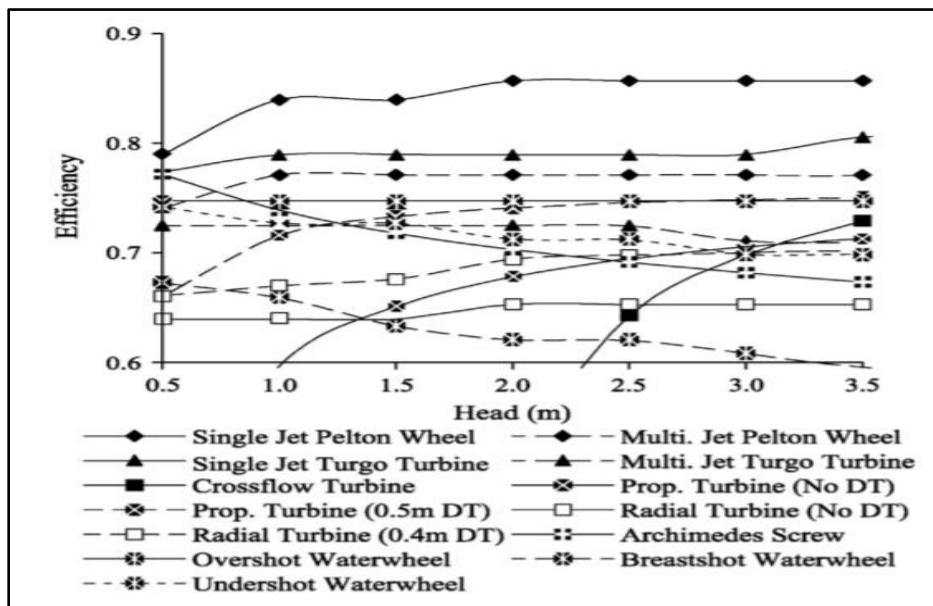


Figure 13: Efficiency variation over head range for different types of hydropower turbines [25]

2.3.2 Solar PV System

A number of individual solar photovoltaic (PV) cells are combined to form a module or panel as shown in Figure 14 (a) and (b). When these cells are connected in series they form a module with a voltage equivalent to the sum of the voltage of individual cells. A number of PV modules can further be connected in series to form a string, and the strings connected in parallel form an array as shown in Figure 15. This means the voltage output of a string is the sum of the voltages of the individual modules while the terminal current remains the same. This is illustrated in Figure 16. On the other hand, modules can be connected in parallel to increase the current output without altering the terminal voltage as depicted in Figure 17. Strings can be connected in parallel to increase the current without increasing the terminal voltage. This combination is shown in Figure 18.

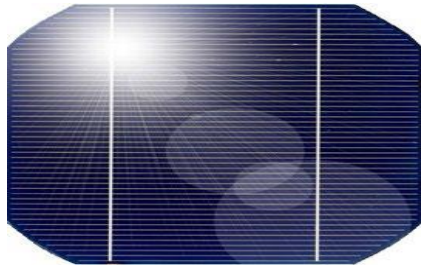
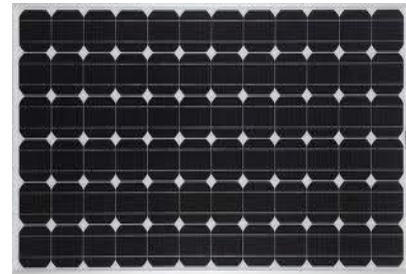


Figure 14 (a): A solar cell



(b): A solar module

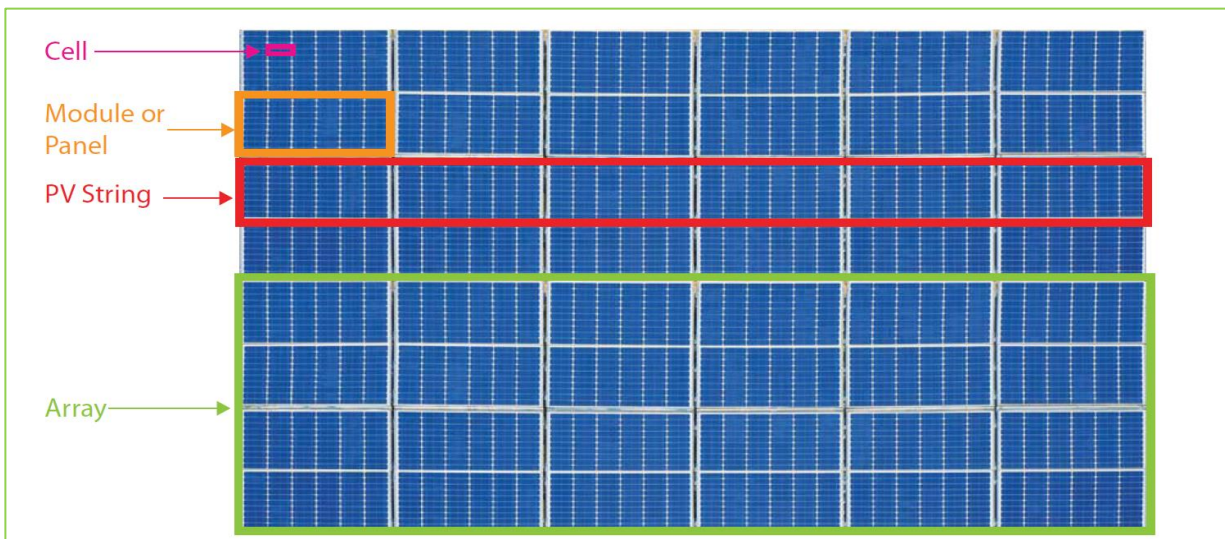


Figure 15: PV module construction

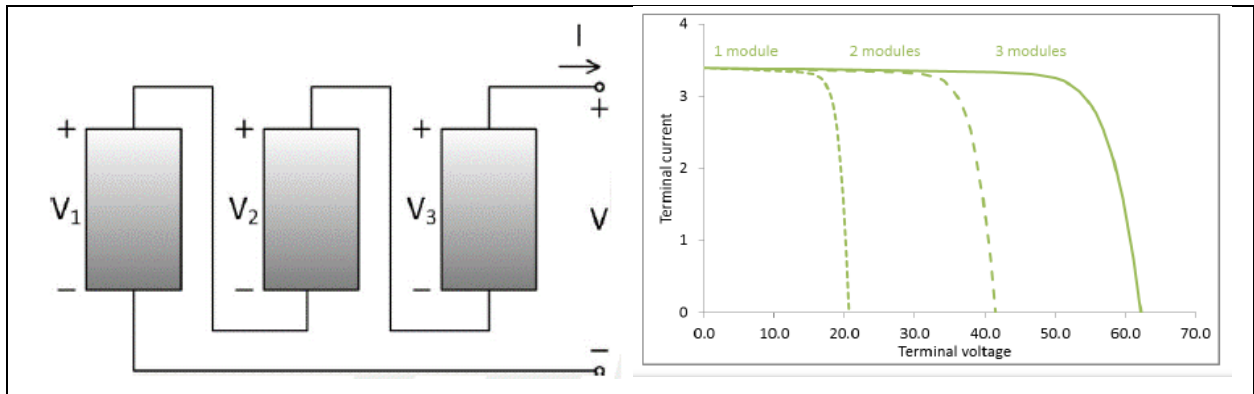


Figure 16: Modules connected in series to form a string

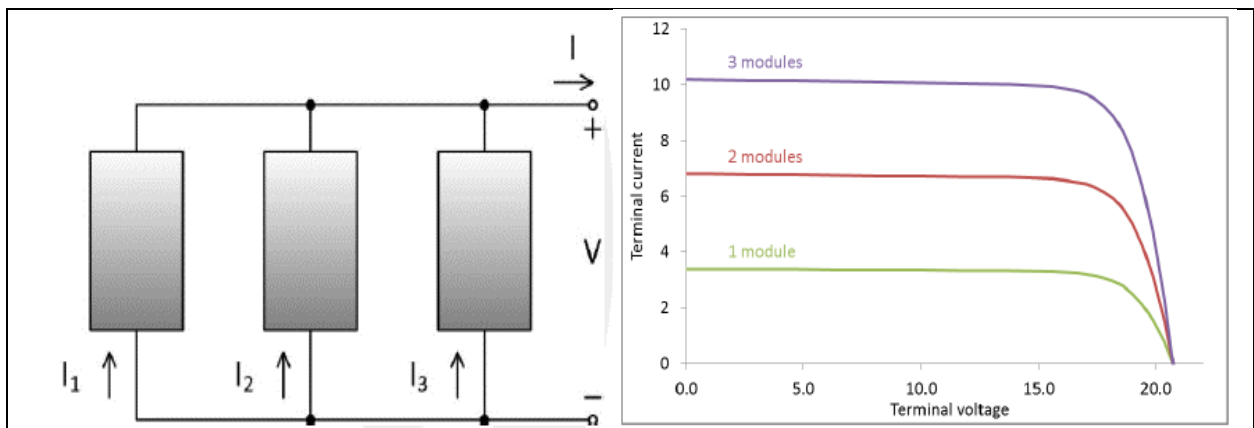


Figure 17: Modules connected in parallel

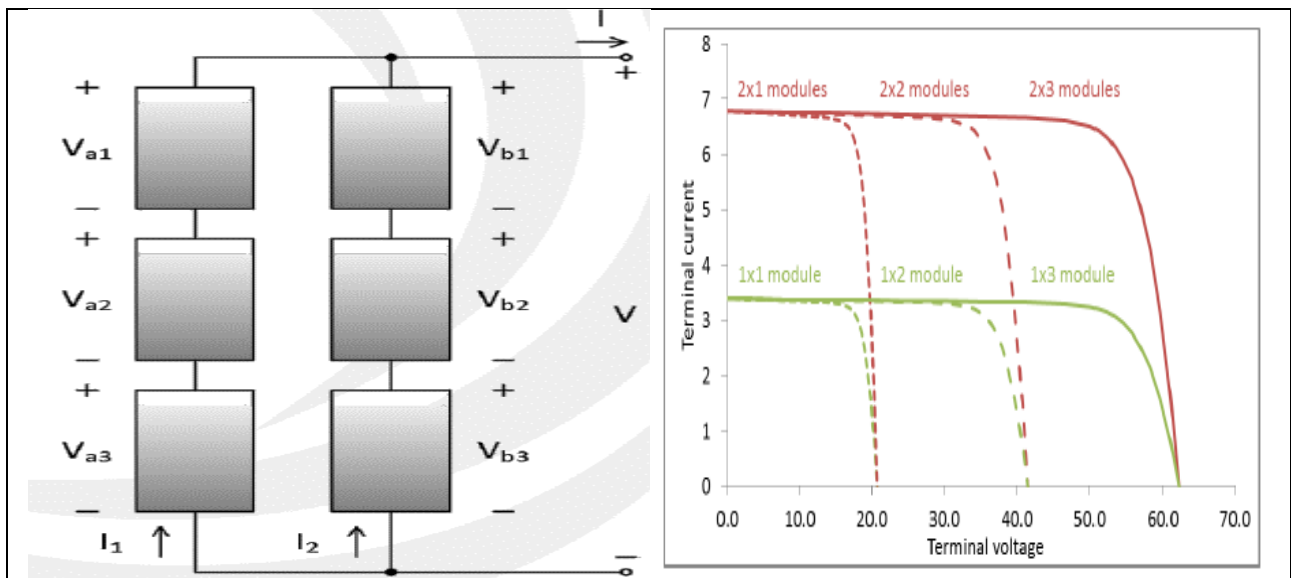


Figure 18: Strings connected in parallel

Photovoltaic cells transform the sunlight directly into electricity. The current produced is determined by the solar radiation intensity that falls on the surface of the cell, while the rise in cell temperature tends to reduce the generated voltage. The Direct Current (DC) produced multiplied by generated voltage equals power, and the power produced by the solar PV panel is calculated using Equation (15) as:

$$P_{pv} = \frac{\eta_{pv}}{\eta_{STC}} \cdot \frac{G_T}{G_{STC}} \cdot P_{STC} \quad (15)$$

where P_{pv} is the PV generator power output in watts (w), η_{pv} is the PV efficiency, η_{STC} is the PV efficiency at Standard Test Condition (STC), G_T is the solar irradiance incident on the plane of the PV array/module in W/m^2 , G_{STC} is the incident irradiance at STC in W/m^2 , P_{STC} is the rated power output of the PV array/module measured at STC.

The operation of a solar cell/module can be expressed graphically with a current (I) voltage (V) (I-V) characteristics curve. This summarizes the relationship between voltage and current at certain conditions of temperature and irradiance. The I-V characteristics curve gives the information required in configuration of a solar system so that it can operate as close as possible to its optimal Maximum Power Point (MPP) [27].

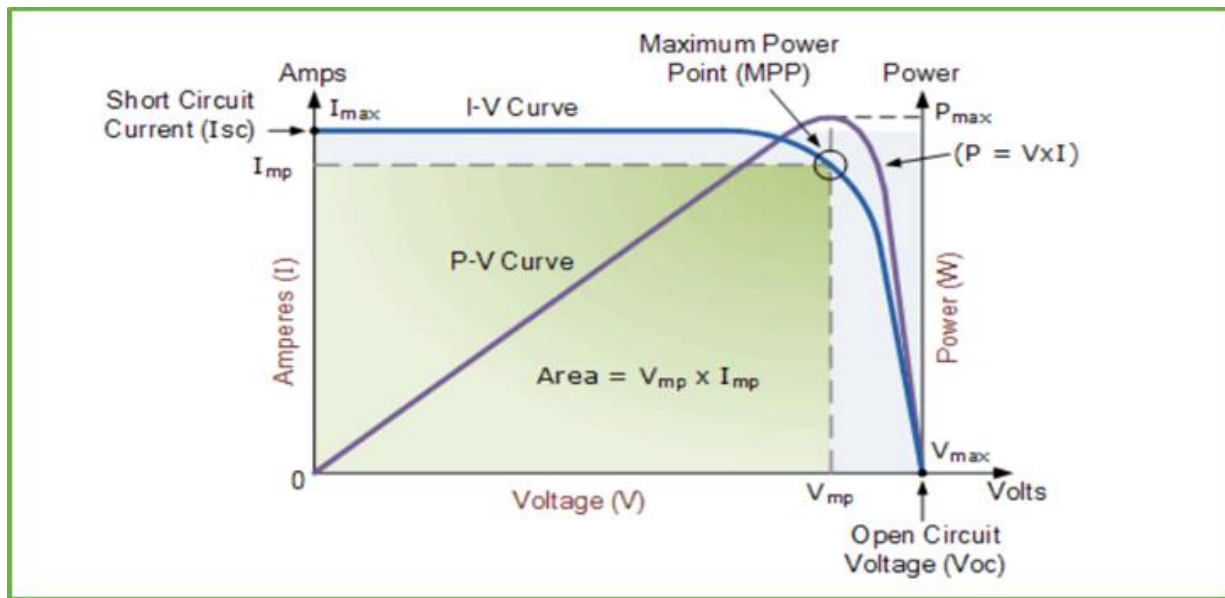


Figure 19: Solar cell I-V Characteristic Curve [28]

The I-V characteristics curve shown in Figure 19 is produced by multiplying a range of voltages from short circuit to open circuit points for a specific radiation level. It can be observed that the range of the curve runs from short circuit current (I_{sc}) at output voltage of zero volts, to zero current at open circuit voltage (V_{oc}). It can be noted that no power is generated at the two extreme points, the power is generated between the two points and the maximum power is being generated at the point somewhere in between, this point is called MPP and is shown at the top right corner of the green rectangle in Figure 19.

2.3.3 Wind Power System

The wind turbines are classified in two main types, the horizontal axis machines and vertical axis machines as depicted in Figure 20. This classification is determined by their axis of rotation. The horizontal axis wind turbines have their axis of rotation parallel to the ground and wind flow. In a number of cases, horizontal axis wind turbines are used for commercial purposes because they have relatively high efficiency and they have an advantage of low cut-in speed [29]. The axis of rotation of vertical wind turbine is vertical, this feature allows the turbine to receive wind from all the direction. The change in wind direction does not require the steering mechanism to rotate the rotor to face the wind. For this type, the gear box and the generator can be installed on the ground. This makes the maintenance to be easier as compared to the horizontal axis machines that have the gear box and the generator mounted in nacelle at the top of the tower [30].



Figure 20 (a): Horizontal axis wind turbine



(b): Vertical axis wind turbine

The Wind Turbine Generator (WTG) is designed to produce maximum power at a wide range of wind speeds. It transforms wind energy into electricity using the aerodynamic force from the rotor blades. As the wind particles flow across the blade, there is air pressure difference between the two sides of the blade. A strong lifting force is created on one side and that causes the rotor to turn, the rotor is connected to the generator and as it rotates it generates electricity. However, the choice of the WTG should be compatible to the project site as the location plays a crucial role in the performance and efficiency of a WTG. The electrical power produced by a wind turbine is given by Equation (16) [31].

$$P = C_p \cdot 0.5 \cdot \rho \cdot A \cdot v^3 \quad (16)$$

where P = power extracted from the wind (W), C_p = power coefficient, ρ = air density, A = swept area (m^2) and v = wind speed at rotor (m/s)

An additional aspect to be considered is the power curve of the wind turbine. The magnitude of the electric power produced by a wind turbine at different wind speeds can be illustrated by the power curve. Typical wind turbine power curve is shown in Figure 21. The turbine starts to rotate and generates power when the wind speed sweeping across the blades reaches the cut-in speed which is normally 3.5 m/s. The generated power increases with the increasing wind speed until the point whereby the wind velocity reaches the rated speed of 14m/s and at this point the wind turbine produces its rated power irrespective of the increase in wind velocity [32].

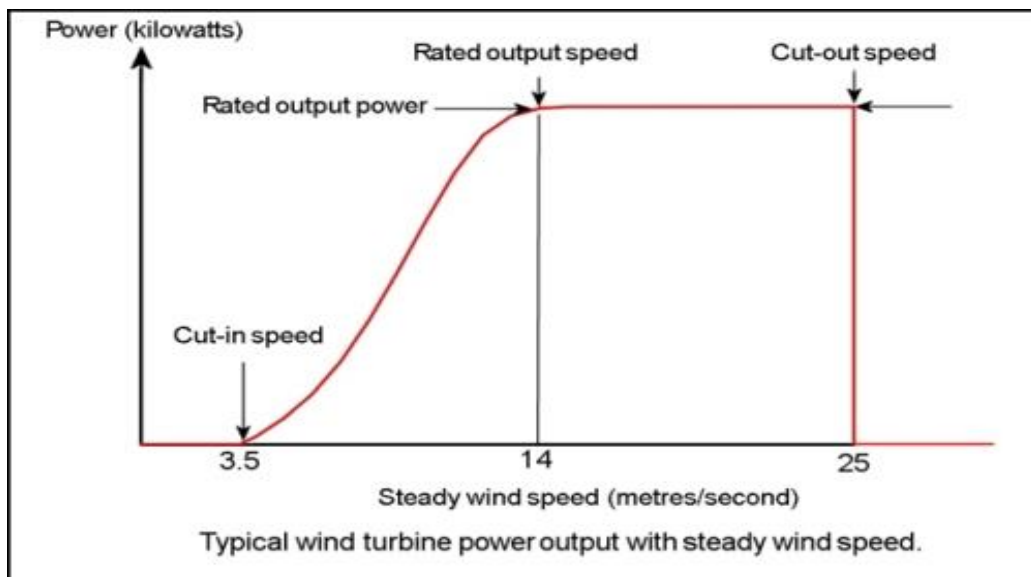


Figure 21: Wind Turbine Power Output Curve [32]

However, if the wind turbine remains operational even beyond its rated wind speed, its efficiency (power coefficient C_p) drops. In simpler terms, the rotor power coefficient can be defined as the ratio of power output to the theoretical power provided by the wind. The power coefficient can be expressed by Equation (17) as:

$$C_p = \frac{2P_T}{\rho_a A_T V^3} \quad (17)$$

Where C_p is the power coefficient, P_T is the turbine power output, ρ_a is the air density, A_T is the rotor cross sectional area swept by the wind, V is the wind velocity.

The manufacturers refer to a wind turbine power curve to give a guarantee to the buyer that the wind turbine generator can produce a specific amount of power at a specific wind speed. Therefore, each location or site is suitable for a certain wind turbine depending on the wind conditions at that site.

2.3.4 Weibull Parameters and Speed Frequency Distribution

The speed frequency distribution can be used to estimate the power output of a wind turbine generator, the potential total energy production on the site, most frequent wind velocity and velocity contributing to maximum energy. It also shows the number of times the wind speed at a study site falls within a certain range or bins. In most cases the range is set at 1 m/s wide with the span from 0 to about 25 m/s and represented as a histogram. The site wind speed frequency distribution is represented by a mathematical function called Weibull distribution or Probability Density Function (PDF) [14]. The Weibull PDF is given by equation (18) as:

$$f(V) = \frac{k}{c} \left(\frac{V}{c}\right)^{k-1} \exp - \left(\frac{V}{c}\right)^k \quad (18)$$

where k is the dimensionless shape parameter, c is the scale parameter in m/s, V is the wind velocity.

Shape parameter indicates the width of the distribution and how the distribution peaked, it shows if the speeds are most of the time close to a certain value. The k values fall between 1 and 3.5, it

reflects how windy the site is on average. As the value of k increases from 1 to higher values, the FDC becomes narrower and that indicates a steadier, less variable wind as illustrated in Figure 22 [33].

2.3.5 Annual Energy Production (AEP) of a wind turbine

The AEP of a wind turbine refers to the overall energy production in kWh or MWh over a period of one year. To get this value, a wind turbine power curve is used. With reference to Figure 23 (a), all the powers for each wind speed are added together [34]. As an example, a wind turbine produces 1 MW at a wind speed of 8.5 m/s, while a wind speed of 9.5 m/s produces a power of 1.5 MW and 2 MW is achieved at the speed around 11 m/s. Therefore, the total production is 4.5 MW, but since the wind speed is distributed over a year as shown in Figure 23 (b), the annual production can be precisely estimated using a PDF [35]. For instance, the wind speed of 8.5 m/s takes place 5.5% of the time in a year and produces the power of 1 MW. This means the energy production at this particular speed is 1 MW multiplied by 5.5% of number of hours in a year (8760) which gives 481.8 MWh/year.

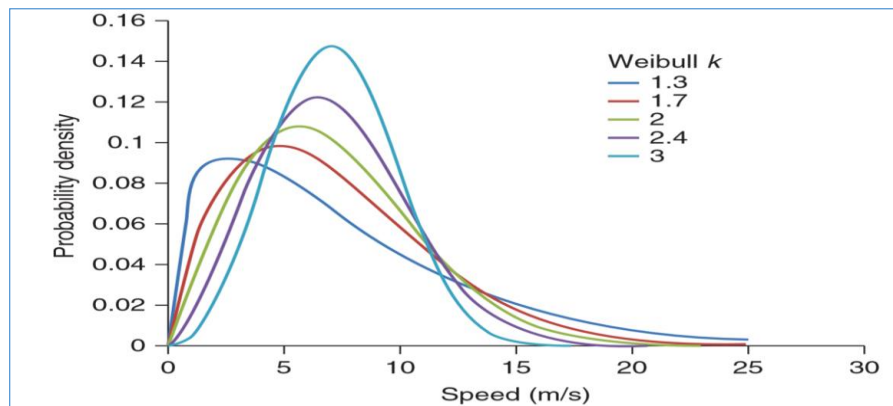


Figure 22: Weibull probability density curves for a range of values of k [33]

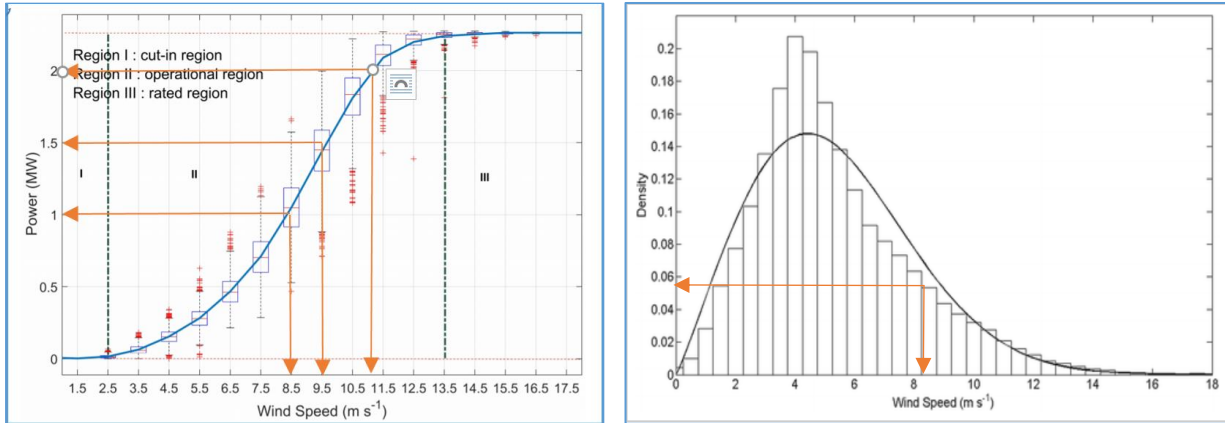


Figure 23: (a) Wind turbine Power curve (b) Probability Density Function (PDF)

A wind turbine generator consists of rotor blades, rotor hub, gearbox, generator and tower as depicted in Figure 24 [36]. The main function of the rotor is to transform wind energy into mechanical energy through the shaft to the gearbox and finally to the generator. The nacelle is the wind turbine housing which protects the turbine components from atmospheric weather conditions and suppresses noise from transmitted mechanical sound. A horizontal axis wind turbine has a yaw system that turns the nacelle clockwise or anticlockwise to the actual wind direction using a yaw motor and yaw drive. Yaw drive rotates the nacelle to keep the rotor facing the direction from which wind is blowing.

Wind turbines should be completely stopped using brakes during the periods of extremely high winds for safety. The gearbox is a component that increases/decreases the rotational speed, therefore in wind turbines it is used to control the generator speed. The generator transforms the mechanical energy to electrical energy. The main function of the tower of a horizontal axis wind turbine is to allow wind energy utilization at sufficient heights above the ground. Some towers are made of steel, some with concrete. The anemometer is a sensor that measures the speed while the wind vane is a sensor that detects the wind direction.

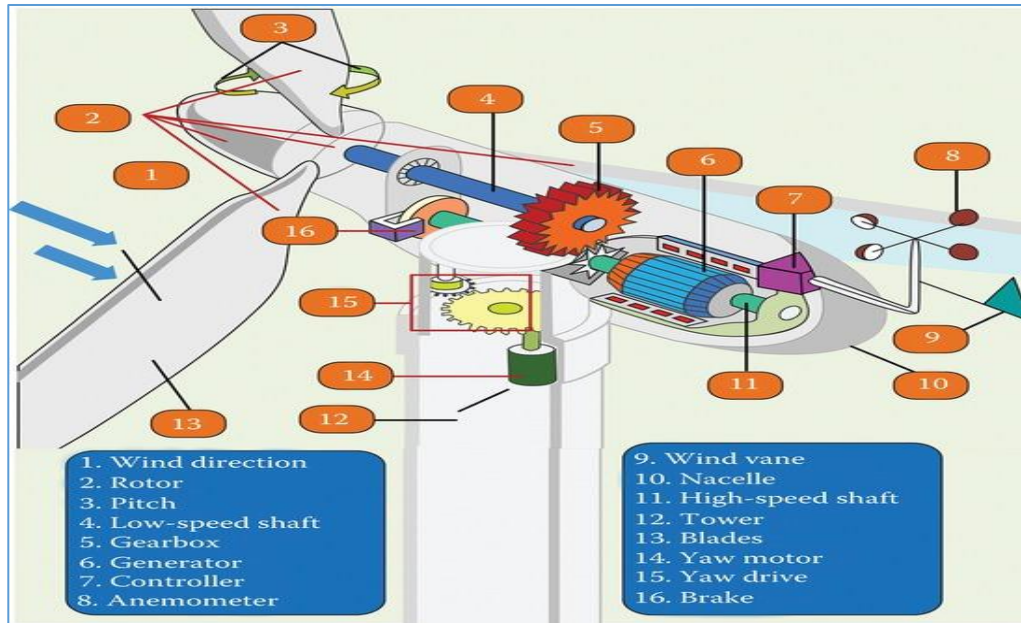


Figure 24: Wind Turbine Generator Components [36]

2.4 Optimization of Hybrid Renewable Energy Systems

This subsection presents a discussion of the relevant literature regarding the implementation and optimization of off grid and grid connected HRES. Another essential point is to review previous literature on success factors and challenges faced by countries which implemented similar HRES. It is important to identify factors that affect a smooth and successful implementation of HRES because the knowledge acquired will help other developers to engage proper strategies for implementation of sustainable systems.

A study on HRES was performed in Benin Republic, driven by a relatively low electrification rate of 30.4% [37]. The electrification rate in rural areas was estimated at 6.9% and 54.5% for urban areas. The main reason for poor grid extension was found to be the high investment required to extend grid to rural areas as well as the low profit margins for the utilities. Similar to Lesotho, Benin Republic had been relying mostly on imports from neighboring countries like Nigeria, Togo and Ghana. The imported power was ranging between 75% and 95% of the local demand [37]. It can be seen from Figure 25 that the imports gradually increased throughout the years with a very small improvement in local production.

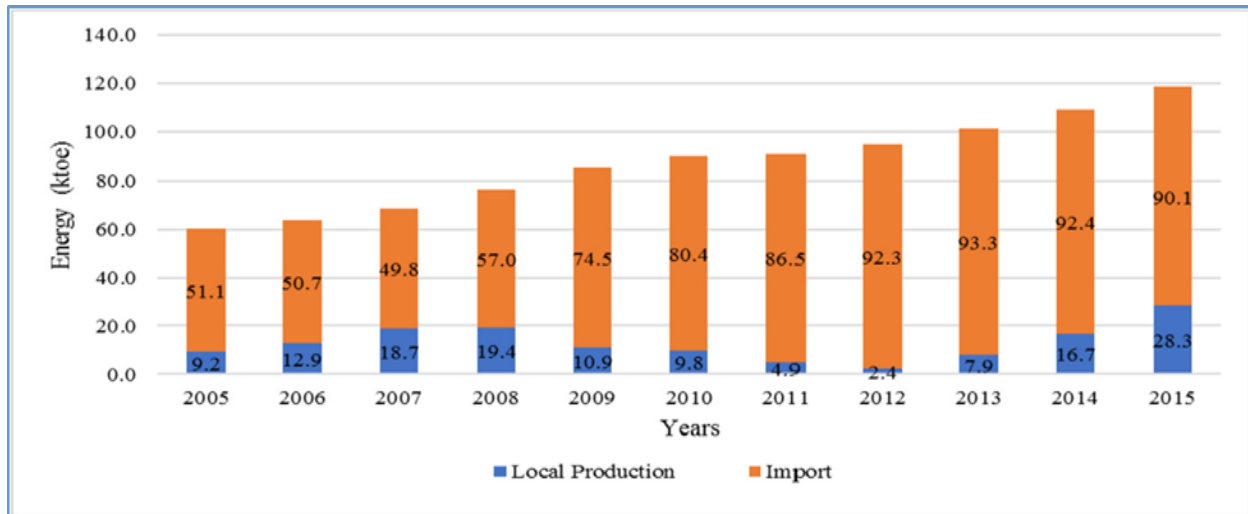


Figure 25: Benin's electricity supply (2005–2015): national production vs. import [37]

In an effort to address the shortage of local production, Benin Republic exploited the untapped RE resources which could improve the demand supply gap and increase the local electricity generation. The most feasible and environmentally friendly configuration was found to be solar PV-diesel generator-battery, this combination was far more economical than extending the grid. This system produced less emissions at only 3% due to high RE penetration of 96.7% [37]. To a certain extent the new system improved the health of the community with regard to possible respiratory problems that would probably affect the local population in a long run. In addition to that, the local community gained access to clean and affordable energy. Figure 26 shows a similar trend to that of Benin Republic whereby the imported energy for Lesotho is increasing gradually every year while the local generation is almost constant. Currently Lesotho's local generation capacity is 72 MW from Muela hydropower station, the additional power to meet the local demand is imported from South Africa and Mozambique. In addition to this, most of the rural areas have no access to electricity due to the mountainous nature of the country which makes the extension of the grid to be extremely difficult and economically not viable [38].

A similar study on simulation and optimization of renewable energy hybrid power system was conducted at Semonkong. It was found that during the dry winter months of June to September, the hydro system is not generating due to lack of water. During this period, only wind and diesel is available for generation. According to this study, the most cost-effective solution for Semonkong was a combination of hydro-wind-diesel-battery with the LCOE of \$0.23/kWh [39]. A similar

study on a grid connected hybrid wind-solar PV-battery was conducted in Navasha Kenya, this part of Kenya experienced frequent power cuts and the introduction of the RE hybrid system improved the reliability of supply to the local community [40]. According to Binayak et al, hybrid renewable energy systems are the most cost-effective intervention where the extension of national grid is expensive, remote rural communities benefit a lot on HRES. A hybrid system comprising of 20 kW hydro, 5 kW solar PV, and 3 kW wind was implemented in remote rural areas of Thingan and Kolkhop, Makawanpur District, Nepal. This hybridization brought about a remarkable improvement in the reliability of supply and the ability to meet the demand for these villages [41].

Year	Energy Purchased (GWh)			Bulk Supply Cost (Million Maloti)	Energy sold (GWh)	Energy loss (%)
	Local	Imports (ESKOM and EDM)	Total Energy Purchased (GWh)			
2013/14	516.4	285	801.44	256.91	705	12
2014/15	515.2	271.2	786.36	265.996	680	16
2015/16	520.8	281.1	801.86	339.07	699	13
2016/17	512.05	373.56	855.61	434.87	743.31	16
2017/18	518.28	373.89	892.17	439.63	778.24	13

Figure 26: Lesotho Electrical Energy purchases and sales [5]

Most of the studies have investigated the optimization and design of off grid hybrid renewable energy system focusing on technical and economic analysis using HOMER software [42]. In the same way, some studies have been conducted to assess the feasibility of HRES. For instance, Aziz et al, carried out a techno-economic feasibility analysis of wind hydro and solar hybrid system and concluded that a combination of two or more renewable energy sources is cost effective especially for areas that experience significant weather variations seasonally [43]. This study did not take into consideration the incorporation of battery storage and analyses the optimal performance of a RE system with a backup battery storage.

In another study, Aziz used HOMER to establish the optimal off grid hybrid system configuration to supply electricity to a desert safari camp. It was discovered that the combination of PV-Wind-

Battery was the best for the study area, when comparing a standalone diesel system NPC with HRES is 1% more. The LCOE for the proposed hybrid system \$0.18/kWh [44]. Lemsomboon et al carried out a feasibility study of HRES that is comprising hydropower, wind technology and PV system for a school located in the remote rural area in Thailand [45]. The outcome of his study revealed that the off-grid hybrid system was a preferred option for rural areas where grid extension is not economically and technically feasible.

A study conducted by Khan et al in South China on performance of the hybrid energy sources combining RESs and conventional sources revealed that the hydro-PV-battery-diesel configuration was the most economical HRES with acceptable amount of carbon emissions, while hydro-diesel system was found to be the second best combination [24]. A similar study to investigate the performance of PV – mini hydro – batteries – wind and a diesel generator hybrid system in Bangladesh was undertaken [46]. The results indicated that this combination compared to others were the best hybrid for the study area. Moreover, Abdulla et al. conducted an economic feasibility study on a grid connected renewable hybrid system and found that hybrid systems incorporating wind technology become feasible at a wind speed of 5.5 m/s or more [12].

Based on the above studies, it is quite clear that the hybrid renewable energy systems are becoming more attractive and popular to most of the researchers as an efficient and alternative approach to address the problem of energy access for rural communities. Although hybrid renewable energy systems come at a higher capital cost, they have an advantage of relatively low operating costs. However, the study conducted by Andreas Coester et al in Germany investigated the impact of large scale battery storage on the security of supply for a grid tie system. Their study revealed that battery storage is necessary for stabilizing the grid and maintaining the continuity of supply, but due to the high cost of batteries the plant would not be profitable unless subsidized [47]. It is obvious from the literature review that most of the researchers have carried out their studies on the similar configurations as considered in this study.

This study investigates the potential of renewable energy resources in the Semonkong area with an isolated mini-grid and the Mantsonyane area connected to the national grid. The focus will be on the addition of solar PV and wind to the existing mini hydropower stations. This is an important implementation because the wind and solar combination is the most promising power generating hybrid due to their complementary nature advantage. It has been discovered that wind speeds are

normally low in periods when the solar resource is at its peak. In the same way, higher wind speeds are experienced in seasons when solar resources are less [48]. While this is the case, these renewable energy sources are highly unpredictable since they entirely depend on climatic conditions. For this reason the reliability of wind and solar hybrid systems can be improved by integrating other sources like battery storage and diesel generator [29].

Reliability of power plants is basically related to how often a plant is operating at its rated power. If a plant operates continuously without interruption then its capacity factor becomes 100% [49]. Even though a diesel generator produces some emissions, in order for a standalone renewable energy system to be more reliable, it is recommended that a diesel generator be included to the system. It has been shown that adding battery storage is more cost effective than having a diesel generator as a backup supply of a HRES. Therefore a PV solar-wind-diesel-battery combination is preferred for standalone system as it is capable of ensuring continuity of supply [50]. On the other hand, the addition of battery storage reduces the hours of operating a diesel generator and that brings down the carbon emissions. Another essential point is that with this combination the PCF improves due to the improved system availability.

The two study areas are located in the remote rural parts of Lesotho, therefore the social, environmental and economic impact of developing such projects on the lifestyle of the community has been taken into consideration in this study. This dimension of analysis is missing in the reviewed literature, but for this study, this type of analysis would be of great significance for the Lesotho policymakers to make an informed decision when it comes to electrification of the similar communities with the same meteorological conditions. It is also important to note that the majority of studies in this field have been conducted on the performance of hybrid systems to establish optimal design with consideration of technical and economic analysis. Despite this, in other studies the analysis was done based on a projected period of certain number of years using the single year data in carrying out the simulation. With this method, the results obtained are extrapolated over the estimated projects lifetime, and this means the performance of the system for all the years is identical to the base year. As a matter of fact, some of the crucial events that may change over the lifetime of the project would have been ignored in this type of approach.

In consideration of the covered literature review, this paper intends to bridge a research gap and provide an optimal design for an off-grid PV – hydro – diesel – wind – battery hybrid system for

Semonkong Lesotho as well as a grid connected PV – hydro – wind hybrid system for Mantsonyane Lesotho. The multi-year data were used to perform simulation for individual years throughout the lifetime of the project. In that manner, most of the critical events like PV deterioration, fuel price variation, and load growth can be accurately modeled and this would not be possible for single year model.

3 CHAPTER 3: RESEARCH METHODOLOGY

This chapter discusses the research methodology that will be followed to design and simulate the HRES for grid connected Mantsonyane mini hydropower station and Semonkong off grid mini hydropower station. As illustrated in Figure 27, different technology options will be chosen for Mantsonyane and Semonkong. A hydro-diesel hybrid system at Semonkong will be modelled to incorporate wind and solar PV technologies and a battery storage. These renewable energy technologies would be arranged in such a manner that there would be a high enough Renewable Fraction (RF) in order to ensure good environmental quality and reduction of emissions from burning of fossil fuels. While a grid connected Mantsonyane hydropower system will be hybridized with, wind, solar PV and battery storage.

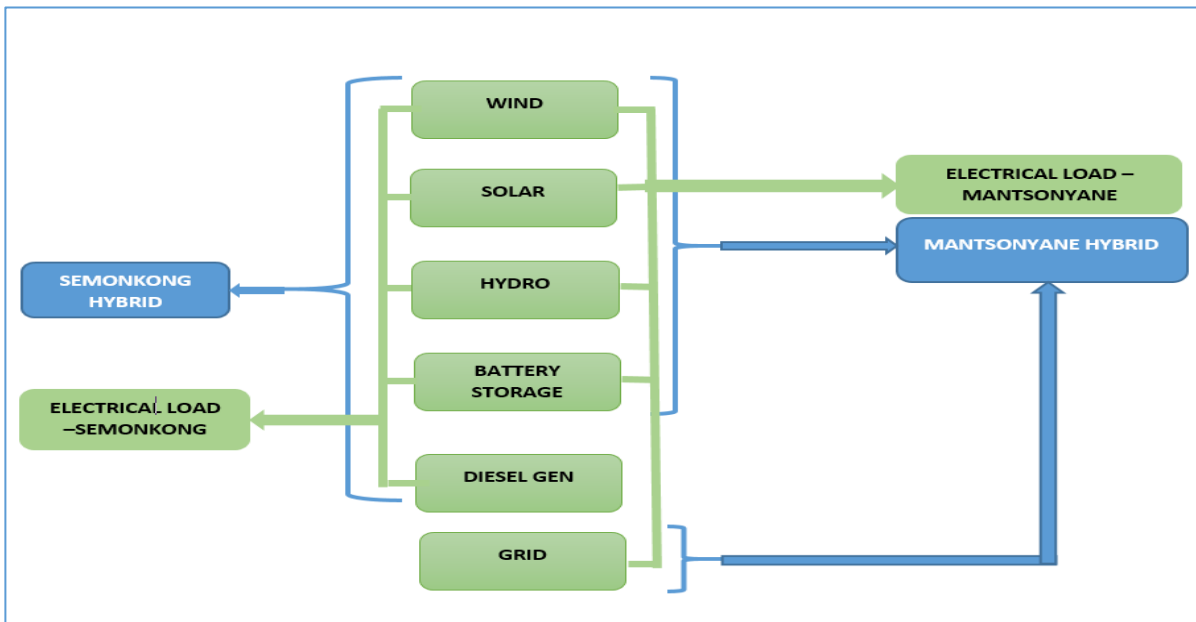


Figure 27: Proposed system configuration

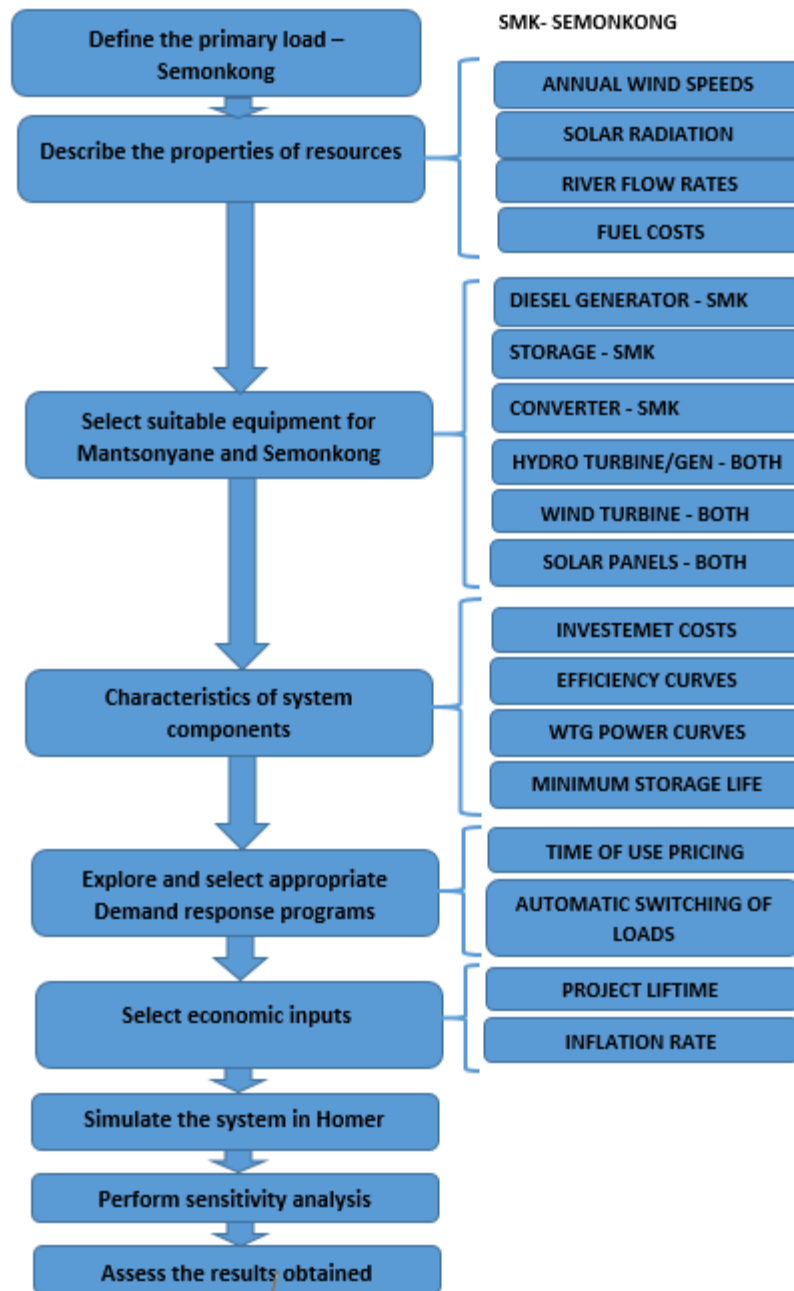


Figure 28: Methodology block diagram

With reference to Figure 28, the definition of primary load for Semonkong and Mantsonyane will be done for the purposes of constructing the load curve for this study. A 30-minutes time step data (kW) for both study areas will be downloaded from the utility’s credit energy meter, the resolution of this data would be converted into energy consumed (kWh) and the resolution will be changed

to 60-minutes time step (hourly data). The Semonkong load profiles will be downloaded from the utility's installed energy meters, as for Mantsonyane mini hydropower station the load demand will be fixed at 2 MW since the objective function is to generate at least 2 MW at any point in time. The existing hydro power plant at Mantsonyane generates only when there is enough water available for generation. If the water levels are too low the system is scheduled to generate between 06:00 and 10:00 then restart at 18:00 and stop at 21:00. During a rainy season when there is abundant water, the plant generates 24 hours.

The following step will be the description of the properties of resources. The solar specific yield (kWh/kW_p/year), the wind yield potential (W/m²) and the river flow rates for Semonkong and Mantsonyane will be established. The next step will be the selection of suitable equipment for Mantsonyane and Semonkong proposed systems, the type of storage, the converter type and size, a suitable type and size of a turbine, generator, wind turbine and solar panels. The next step will be characterization of each component of the system, this includes the investment costs, fuel and efficiency curves, wind turbine generator power curves and CO₂ emissions. This step will be followed by a selection of appropriate demand response program. Selection of economic inputs such as project lifetime and inflation rate will be done. These data will then be fed into HOMER simulation tool to perform simulation and to provide all the possible system configurations. This study will consider the optimal configuration in terms of minimum Levelized Cost of Electricity (LCOE), highest renewable fraction and reliability. Sensitivity analysis will also be conducted to evaluate the impact of variation in some techno-economic factors on system performance.

This study is going to follow quantitative approach to provide a clear explanation of problems to be addressed. In quantitative research method, objective theories are being tested by examining the relationship among variables. Finally these variables can be measured normally by instruments and then analyzed using statistical procedures [51]. Quantitative method is suitable as the study made use of the instrument measured data to establish if there is a potential to generate electricity using wind, solar and hydro, and to compute the optimal capacity of the system. For this research to achieve the objectives, solar irradiation was acquired from NASA. The flow rates data of Mantsonyane River and Maletsunyane River (Semonkong) covering a minimum of ten (10) years has been acquired from the Department of Water Affairs (DWA) while the wind speed for both sides were acquired from Lesotho Meteorological Services (LMS). To measure reliability,

reference to previous studies conducted by consultants is done. Reliability is defined as the degree to which the data collection tools used yield consistent findings similar to the conclusions made by other researchers who implemented similar methods. In the same way, validity is explained as the degree to which the research tools are accurate in measuring what it is intended to measure[52].

3.1 Define the Primary load

The Semonkong load, with the average energy consumption to be met by the proposed system is given as 2,850.33 kWh/d with a peak load of 208.04 kW as illustrated in Figure 39 (a) and the average load of 123.25 kW as shown in Figure 29. It can be seen that the morning peak demand is reached at 6:00 as a result of residents waking up to resume normal activities of turning on the lights and other appliances in preparation to go to their respective work places. The evening peak is attained at around 20:00 due to the fact that most of the people are at home making use of electrical appliances.

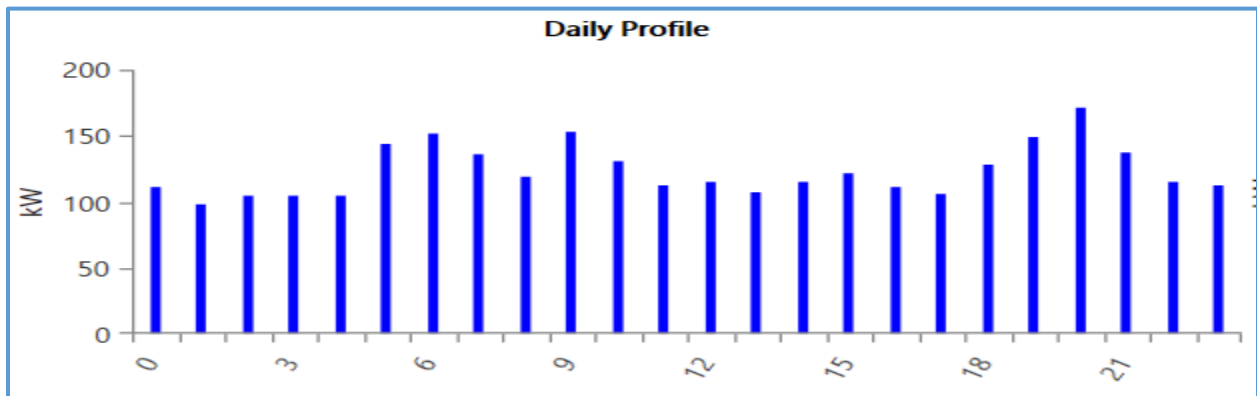


Figure 29: Semonkong daily load profile

The Mantsonyane 2 MW hydropower system is connected to the grid and it is intended to deliver 2 MW or more to the grid. Since Mantsonyane mini hydropower feeds to the grid, it is not necessary to define the load therefore the grid is regarded as the load to be served with at least 48 MWh/day at a peak of 2 MW as shown in Figure 30. Due to variability of hydro resource as a result of frequent severe draughts, the plant is unable to deliver this amount of energy per day. The objective function of the this part of the study is to ensure that the hydro resource is supplemented by other sources of energy to achieve a production of at least 2 MW, all transferred to the grid.

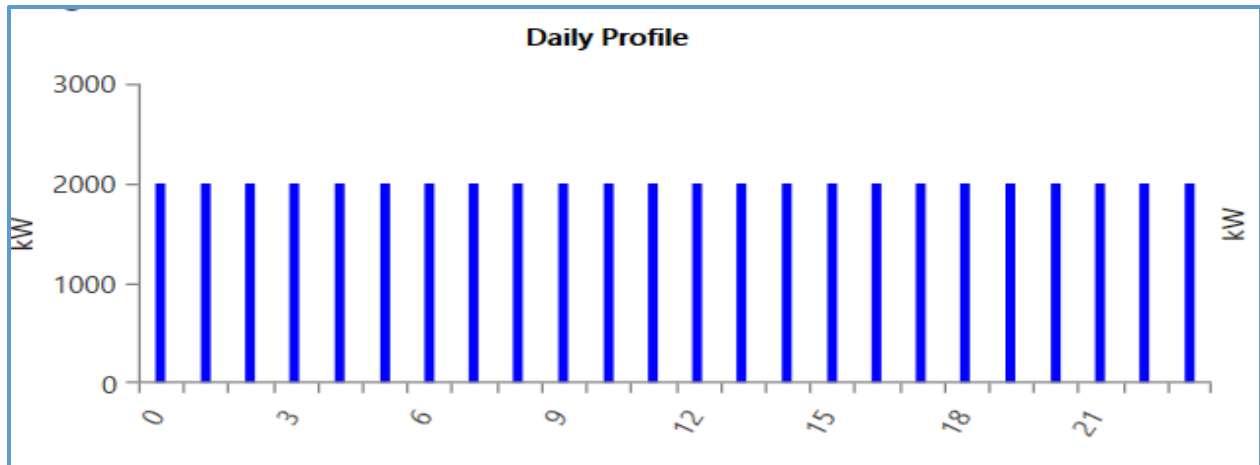


Figure 30: Mantsonyane’s simulated minimum daily load profile

3.2 Undertake Resource Assessment and describe their properties

The following primary renewable energy sources have been considered; hydro, wind and solar. Solar radiation and wind speed for the two study sites were automatically generated with HOMER by inserting the following coordinates for Mantsonyane and Semokong, S 29° 35’ 44”; E 28° 17’ 40” and S 29° 49’ 22” ; E 28° 1’ 39” respectively, and HOMER retrieves the data from National Aeronautics and Space Administration (NASA). The river flow rates data for Mantsonyane and Maletsunyane rivers were obtained from the Lesotho Department of Water Affairs (LDWA).

3.2.1 Solar Resource

The magnitude of PV power generation is primarily influenced by solar radiation and ambient temperature. Figure 31 present the daily radiation and clearness index for Semonkong and Mantsonyane respectively. The two sides show a similar radiation pattern due to the fact that they are not far apart on the solar radiation map. The annual average solar radiation received in Mantsonyane and Semonkong per day is about 5.44 kWh/m²/day with a maximum solar radiation of 7.02 kWh/m²/day. The monthly clearness index varied between 0.571 in February and 0.702 in July with an annual average of 0.626. Clearness index shows the level of the presence of solar radiation on the surface of the earth as well as variations in atmospheric and weather condition at a site. Clearness index can also be explained as the portion of solar radiation at the top of the atmosphere that falls on a particular point on earth [53]. Considering the range of values of the clearness index, the Mantsonyane and Semonkong weather conditions can be classified as partly overcast. It can be noted that the two areas experience a reasonable amount of solar radiation and

this confirms that usage of PV system can be given a favorable consideration. The two study sites similarly show higher levels of solar radiation from August to April and lower levels from May to July.

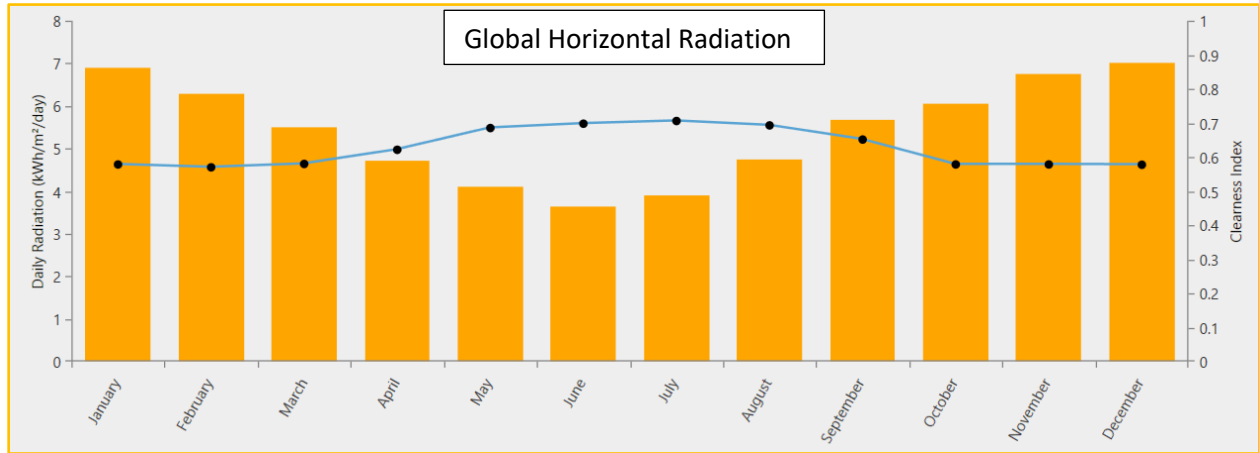


Figure 31: Semonkong and Mantsonyane’s daily radiation and clearness index

3.2.2 Hydro Resource

It is highly critical to select a site that has abundant stream water throughout the year in order to have a reliable water supply to the hydropower systems. Meltwater from snow, rainfall water sources and small rivers upstream contribute to the reliability of water supplies to the project site [13]. The average monthly stream flows for Mantsonyane River were computed from the year 2000 to 2015 as depicted in Figure 32. Due to huge data gaps identified in 2006, 2007, 2010 and 2011, these years were not included in the assessment process. It can be seen that the average stream flows are comparatively lower in winter months (April to July).

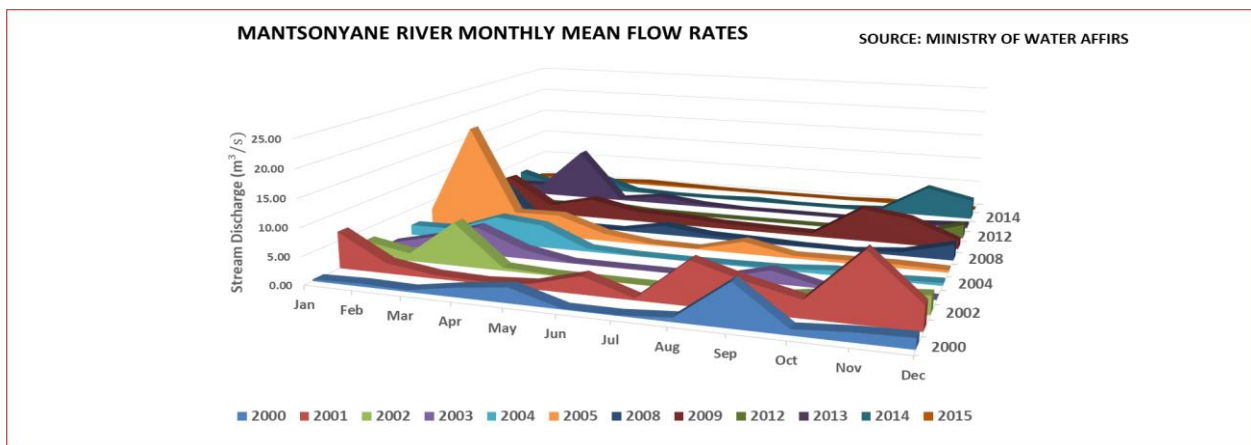


Figure 32: Average monthly streamflow for Mantsonyane River

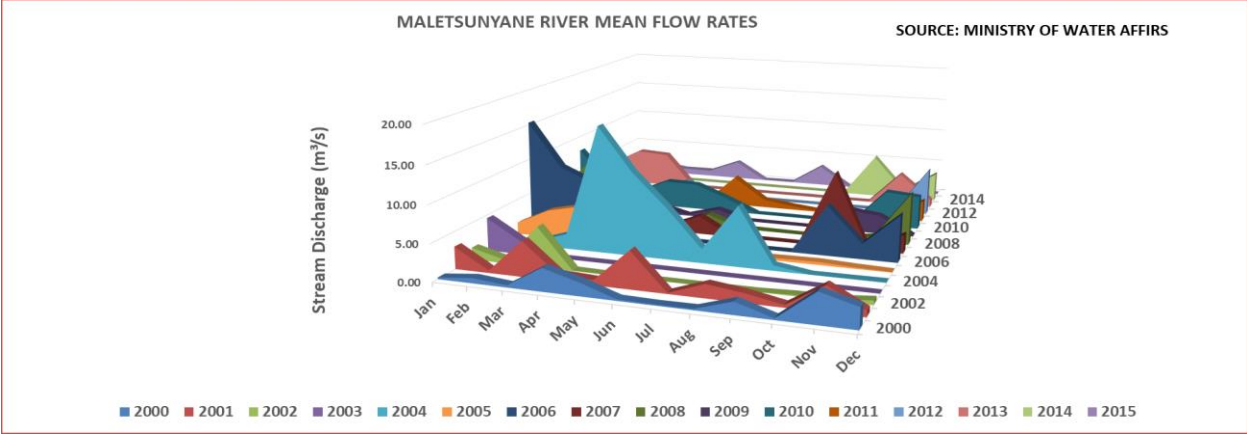


Figure 33: Average monthly streamflow for Maletsunyane River

In addition, the average monthly stream flows for Maletsunyane River were calculated from the year 2000 to 2015. It can be seen that winter experienced low rainfall as it is indicated by low stream discharge during this season. The year 2004 is the outlier with a comparatively high discharge from March up to September and this suggest that there was abundant rain in that year.

Figure 34 and Figure 35 illustrate the monthly average stream flow for Maletsunyane and Mantsonyane rivers respectively. The collected data for Maletsunyane River show that the monthly average stream flow varies between 227.184 L/s and 2,917.17 L/s with an annual average flow rate of 1,674.93 L/s. The Mantsonyane River monthly average flow rate varies between 239 L/s to 3,974 L/s with annual flow rate of 1,731.25 L/s. Since both Semonkong and Mantsonyane hydropower plants are designed based on average flow during the year, then it would be uneconomical to keep them online once the flow falls below the design flow rate. In order to mitigate that problem, the flow constraints were considered and defined in Figure 49 and Figure 51.

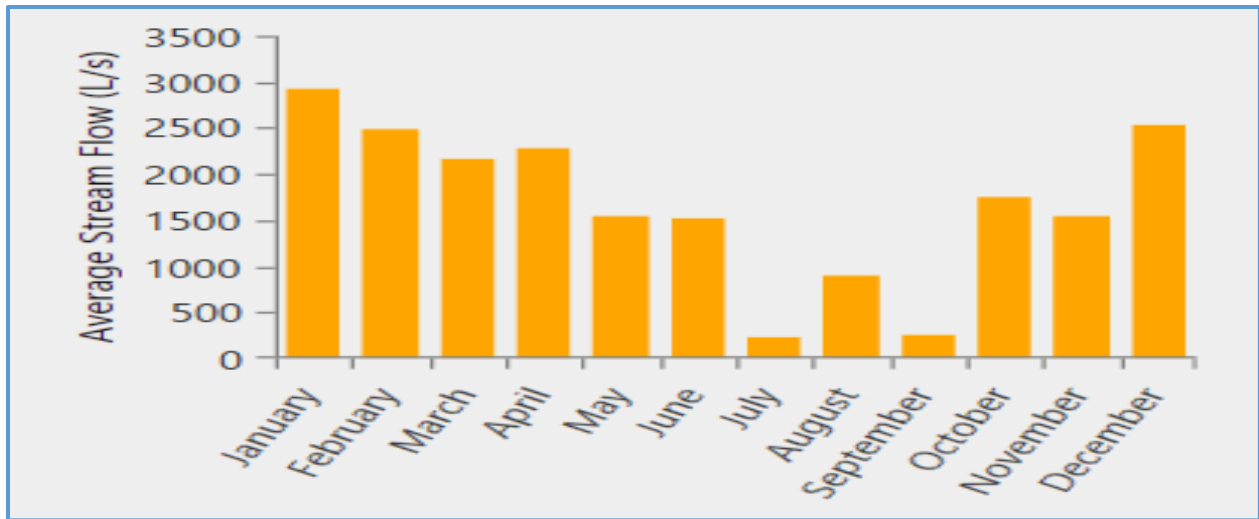


Figure 34: Monthly Average streamflow for Maletsunyane River (15 years)

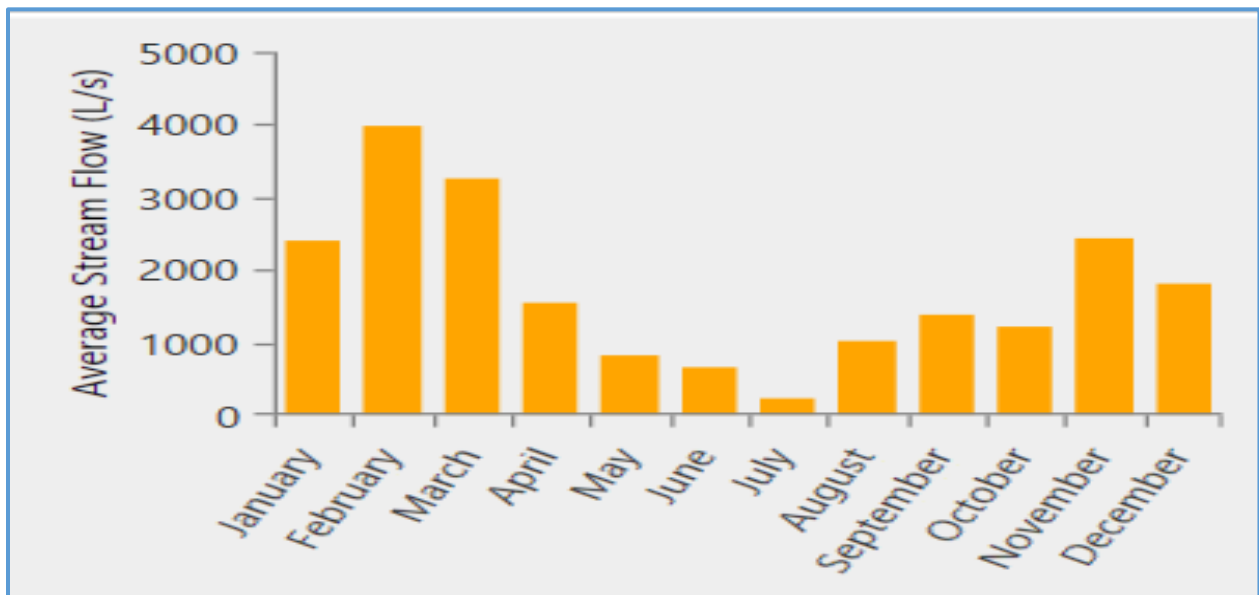


Figure 35: Monthly Average streamflow for Mantsonyane River (12 years)

3.2.2.1 Flow Duration Curve (FDC)

The combination of Maletsunyane River FDC and power curve is illustrated in Figure 36. The power curve shows power output of the installed generator at Semonkong mini hydropower station. The Semonkong system rated discharge is $1.2 \text{ m}^3/\text{s}$ with the rated head of 18 m, equation (9) with the overall efficiency of 90% was used to calculate power generated and to plot the power curve points at different flow rates. It can be observed that the power output increases sharply from

Q₁₀₀ to Q₇₅ flow rate. As the stream flow increases beyond the rated flow of 1.2 m³/s at Q₇₅ the power output does not increase anymore, it remains at a rated power of 180 kW. This behavior explains that the rated flow is equaled or exceeded for 75% of the time, in other words the system should be able to operate at its rated capacity for 75% of the time.

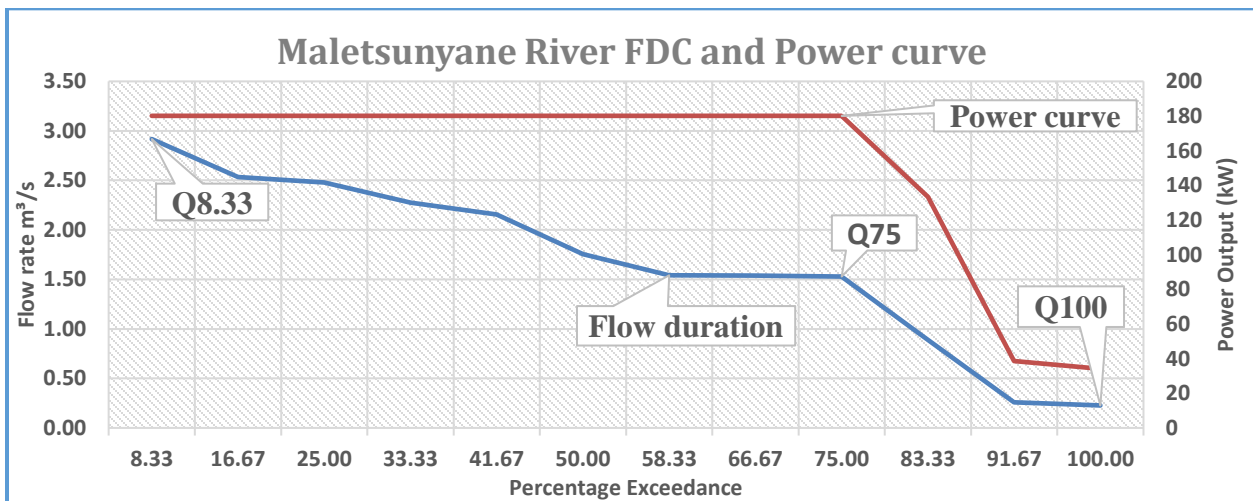


Figure 36: Maletsunyane River FDC and Power curve

The combination of Mantsonyane River FDC and power curve is illustrated in Figure 37, the power curve shows power output of the installed generator at Mantsonyane mini hydropower station. This system is designed to produce the rated power of 2 MW at a rated discharge of 6.5 m³/s with the rated head of 35.5 m. With reference to Figure 37 it is seen that the unit never attains its rated

power due to the fact that the maximum stream flow is slightly less than the rated discharge of the turbine. The maximum power produced is 1,176.38 kW at $Q_{8.33}$. This means that this plant is able to produce 1,176.38 kW for only 8.33% of 8,760 hours which gives about 730 hours in a year.

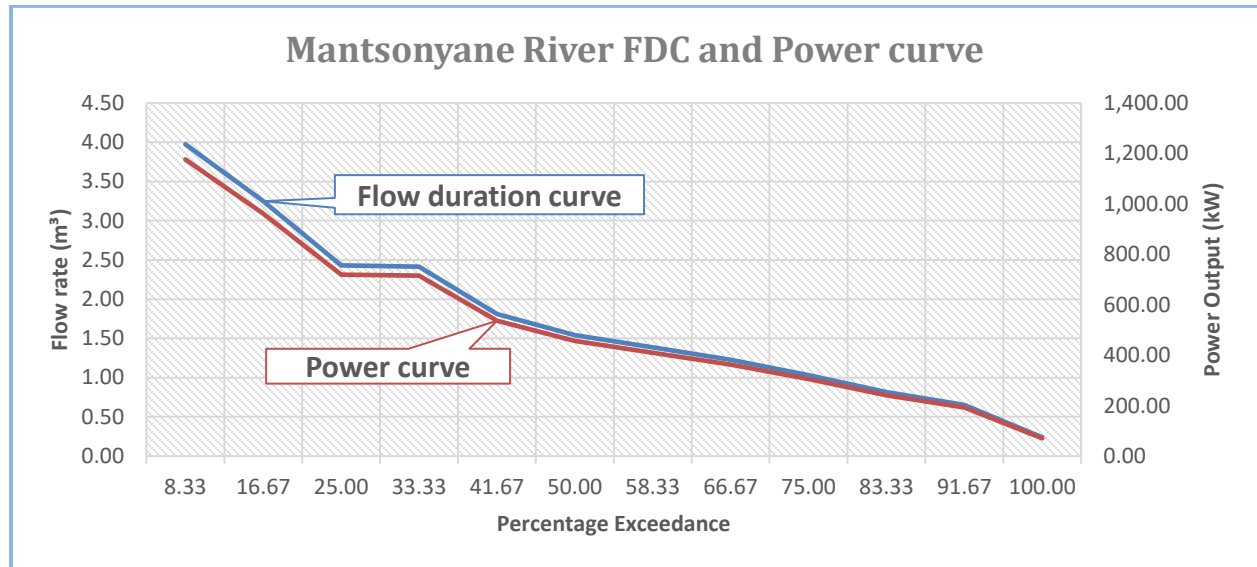


Figure 37: Mantsonyane River FDC and Power curve

3.2.3 Wind Resource

The monthly wind speed of Semonkong and Mantsonyane is illustrated in Figure 38 . It can be seen that the wind speed varies from month to month. The wind speeds at these two sides were taken at anemometer height of 10m and was extrapolated to the turbine hub height of 38 m using equation (3). The extrapolated wind speed was fed into HOMER for simulation. The annual average wind speed at Semonkong and Mantsonyane is 9.71 m/s. Due to the nature of low wind speed at these sites, wind turbine generators with a low cut-in speed of 3.0 m/s were selected. The effects of varying wind speed on the performance of the turbine was investigated by performing a sensitivity analysis on a range of wind speeds. The wind speed was varied in the following manner 6 m/s, 9.71 m/s and 12 m/s

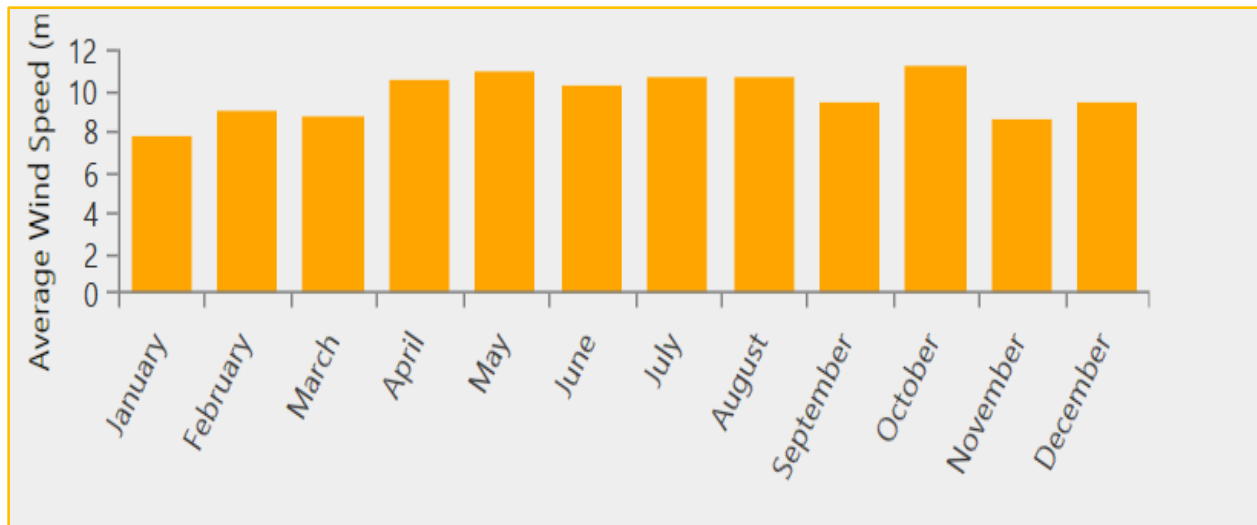


Figure 38: Average wind speed at Semonkong and Mantsonyane

3.2.4 Diesel Fuel

The diesel fuel local price used in this study is \$1 per litre. The effects of diesel price on the optimal performance of a hydro-wind-PV-Diesel generator-battery hybrid system and electricity cost were investigated by varying diesel price in the following manner \$0.5/L, \$ 1.0/L and \$1.5/L. The highest price of \$ 1.5/L may cater for transportation of diesel from Maseru to Semonkong. It should be noted that about 600 L of diesel are used every day in winter and about 400 L/day in summer season, this is according to the plant operators at Semonkong mini hydropower plant.

3.3 Hybrid system components and Specifications

In this study, the following major components are considered for Semonkong hybrid system: PV module, batteries, inverter, wind turbine generator, mini hydro turbine, and diesel generator as shown in Figure 39 (a). The following are considered for Mantsonyane hybrid system: PV module, inverter, wind turbine generator, and mini hydro turbine and battery storage as illustrated in Figure 39 (b).

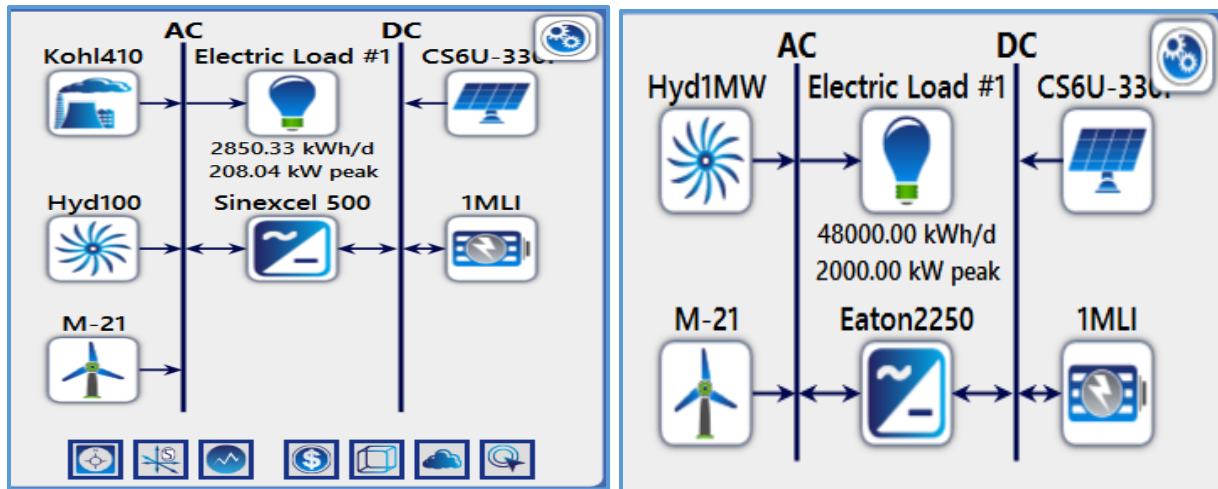


Figure 39: (a) Semonkong Hybrid system modelling (b):Mantsonyane Hybrid system modelling

3.3.1 Selection of suitable equipment for Semonkong and Mantsonyane

For each component in the proposed hybrid system of Semonkong and Mantsonyane, different input parameters such as size, lifetime and costs are specified in details. Table 1 illustrates the technical specifications of all the major system components.

3.3.1.1 Solar PV module

The cell module number CS6U-330P poly-crystalline Canadian solar PV module with 72 (6x12) Poly-crystalline cells with a rated power of 330 W_p is used. The solar farm modules are intended to be mounted on a fixed axis facing North, at latitude -29.7° . The cost of a solar PV module is determined by its physical size, power rating, technology, the brand and country of purchase. The capital cost of a selected solar PV module at study time (December 2019) was \$0.40/Watt [54].

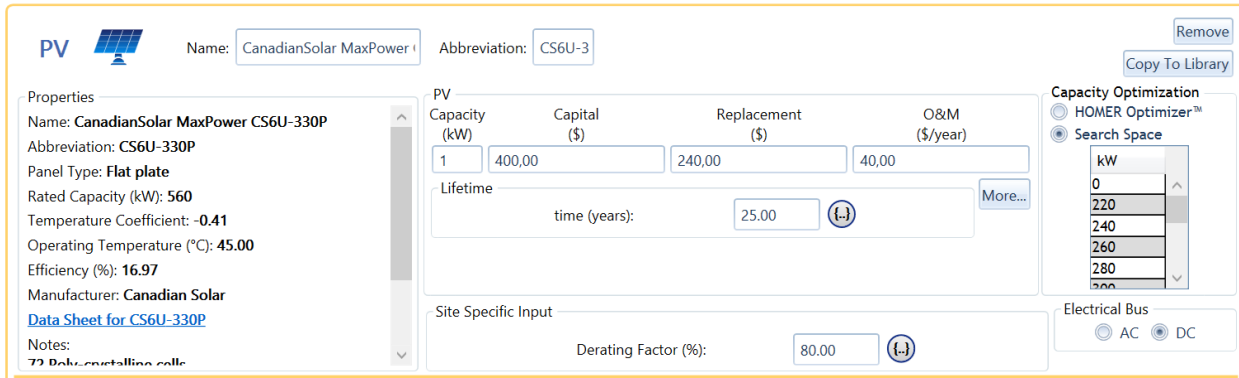


Figure 40: Solar PV module (Semonkong)

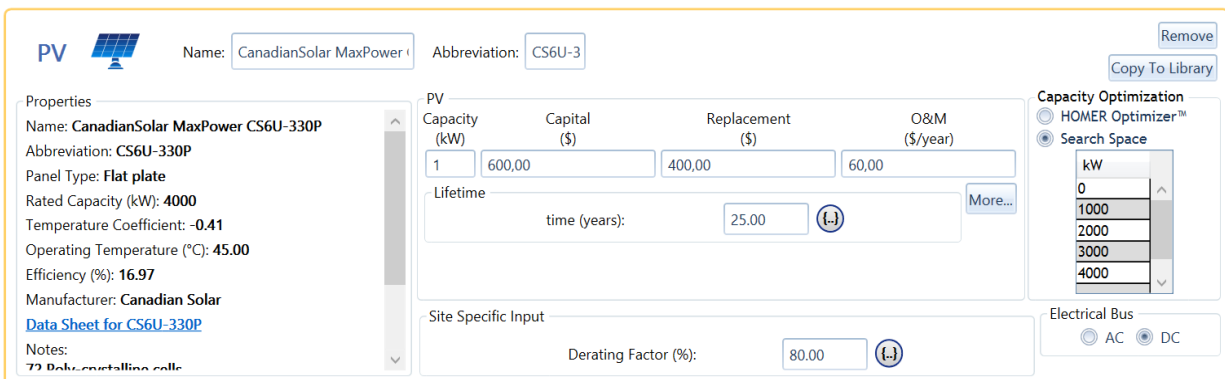


Figure 41: Solar PV module (Mantsonyane)

3.3.1.2 Wind turbine generator

In this study, the XANT M-21 model wind turbine is preferred. This model is designed to operate at hub height of up to 38 m high with the cut-in wind speed of 3 m/s and the rated wind speed of 11 m/s [55]. The power curve, annual yield and recommended hub height for this wind turbine are presented in Figure 42. Figure 43 shows the Weibull PDF with a shape parameter (k) of 2 and a scale parameter (c) of around 10.5 m/s. The average wind speed at both the study sites is around 9.71 m/s, at this speed the XANT M-21 can deliver 480 MWh/annum as per the manufactures specifications. Since the wind speed varies throughout the year, it can be seen that the speed of 9.71 m/s occurs for only 7.8% of the time in a year at the study site therefore the actual production at this site would be 7.8% multiplied by 8760 hours in a year. This gives 683 hours, so the energy produced would be 328 MWh/annum. The capital cost of this turbine is taken as \$70,000.00 [56]. The replacement cost is estimated at \$70,000.00, Operation and Maintenance (O&M) cost is estimated at 5% of the capital cost.

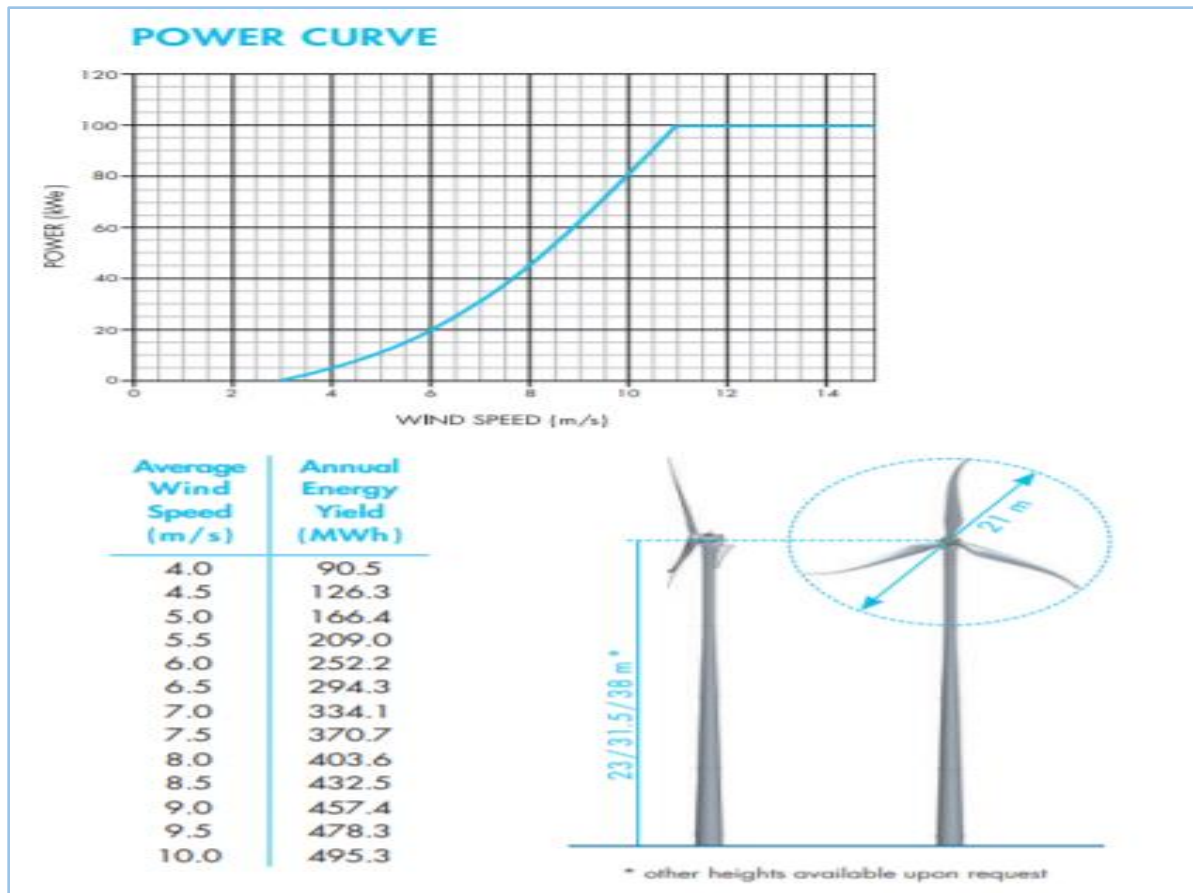


Figure 42: Power curve and annual yield of XANT M-21 wind turbine model [55]

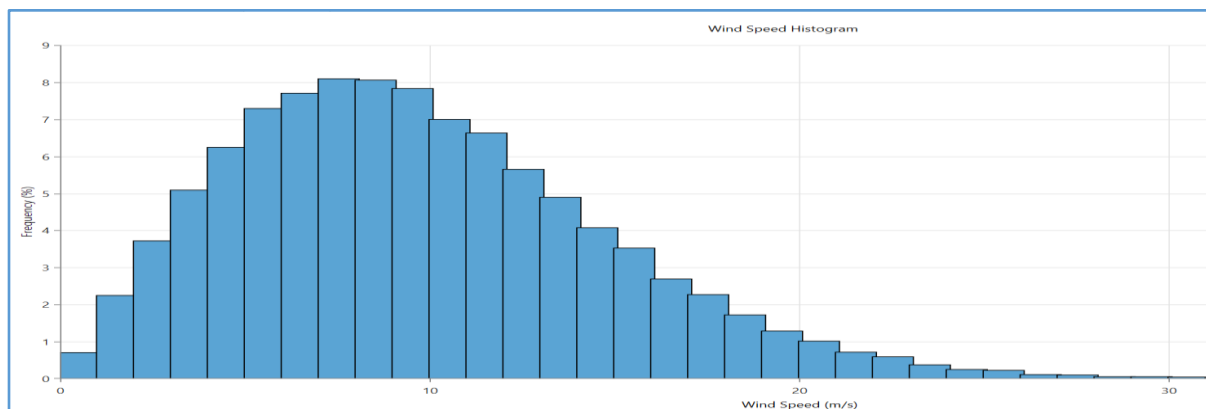




Figure 43: Semonkong and Mantsonyane’s wind speed PDF

WIND TURBINE  Name: XANT M-21 [100kW] Abbreviation: M-21 Remove
Copy To Library

Properties
Name: XANT M-21 [100kW]
Abbreviation: M-21
Rated Capacity (kW): 100
Manufacturer: XANT 

Costs

Quantity	Capital (\$)	Replacement (\$)	O&M (\$/year)
1	\$70 000,00	\$70 000,00	\$3 500,00

Click here to add new item

Multiplier:


Site Specific Input
Lifetime (years): Hub Height (m): Consider ambient temperature effects?


Quantity Optimization
 HOMER Optimizer™
 Search Space

Quantity:

Electrical Bus
 AC DC

Figure 44: Wind turbine generator (Mantsonyane)

WIND TURBINE  Name: XANT M-21 [100kW] Abbreviation: M-21 Remove
Copy To Library

Properties
Name: XANT M-21 [100kW]
Abbreviation: M-21
Rated Capacity (kW): 100
Manufacturer: XANT 

Costs

Quantity	Capital (\$)	Replacement (\$)	O&M (\$/year)
1	\$70 000,00	\$70 000,00	\$3 500,00

Click here to add new item

Multiplier:

Site Specific Input
Lifetime (years): Hub Height (m): Consider ambient temperature effects?

Quantity Optimization
 HOMER Optimizer™
 Search Space


Quantity:


Electrical Bus
 AC DC

Figure 45: Wind turbine generator (Semonkong)

3.3.1.3 Battery

A lithium ion battery storage is used in this study. The capital cost of the battery storage is taken at \$30,000.00 [57]. The replacement cost is estimated at \$20,000.00, Operation and Maintenance (O&M) cost is estimated at 1% of the capital cost.

STORAGE  Name: Generic 1MWh Li-Ion Abbreviation: 1MLI Remove
Copy To Library

Properties
Idealized Battery Model
Nominal Voltage (V): 600
Nominal Capacity (kWh): 1E+03
Nominal Capacity (Ah): 1.67E+03
Roundtrip efficiency (%): 90
Maximum Charge Current (A): 1.67E+03
Maximum Discharge Current (A): 5E+03
www.homerenergy.com
This is a generic lithium ion battery package with 1 MWh of energy storage.


Batteries

Quantity	Capital (\$)	Replacement (\$)	O&M (\$/year)
1	30 000,00	20 000,00	300,00

Lifetime
time (years):
throughput (kWh):

Site Specific Input
String Size: Voltage: 600.00 V
Initial State of Charge (%):
Minimum State of Charge (%):

Quantity Optimization
 HOMER Optimizer™
 Search Space

#

Figure 46: Storage battery (Semonkong)

STORAGE

Name: Generic 1MWh Li-Ion Abbreviation: 1MLI

Properties
Idealized Battery Model
 Nominal Voltage (V): 600
 Nominal Capacity (kWh): 1E+03
 Nominal Capacity (Ah): 1.67E+03
 Roundtrip efficiency (%): 90
 Maximum Charge Current (A): 1.67E+03
 Maximum Discharge Current (A): 5E+03

www.homerenergy.com
 This is a generic lithium ion battery package with 1 MWh of energy storage.

Batteries

Quantity	Capital (\$)	Replacement (\$)	O&M (\$/year)
1	30 000,00	20 000,00	300,00

Lifetime
 time (years): 15.00
 throughput (kWh): 3 000 000.0

Quantity Optimization
 HOMER Optimizer™
 Search Space

Site Specific Input
 String Size: 1 Voltage: 600.00 V
 Initial State of Charge (%): 100.00
 Minimum State of Charge (%): 10.00

Figure 47: Storage battery (Mantsonyane)

3.3.1.4 Converter

A three-phase bidirectional dual mode hybrid inverter has been selected for this study, this inverter is capable of being used with multiple renewable energy sources in both DC coupling and AC coupling such as solar PV, mini hydro generator and wind turbine generators. The cost of the inverter is taken as \$85.00/Kw with the replacement cost of \$75.00. the O&M is estimated at \$8.5 [58].

CONVERTER

Sinexcel 500kW

Name: Sinexcel 500kW Abbreviation: Sinexcel

Properties
 Name: Sinexcel 500kW
 Abbreviation: Sinexcel 500
www.sinexcel.us
 Notes: Both gri-forming and following

Costs

Capacity (kW)	Capital (\$)	Replacement (\$)	O&M (\$/year)
1	\$85,00	\$75,00	\$8,50

Click here to add new item

Capacity Optimization
 HOMER Optimizer™
 Search Space


Site Specific Input
 Inverter Input: Lifetime (years): 10.00, Efficiency (%): 97.67
 Rectifier Input: Relative Capacity (%): 100.00, Efficiency (%): 97.67
 Parallel with AC generator?

Figure 48: Semonkong hydro power station – Sinexcel 500 Converter

3.3.1.5 Mini hydro turbine

The existing water turbine at Semonkong plant is a horizontal axis Francis turbine with a power rating of 180 kW. The design flow rate is 1,200 L/s and the net head is 18 m. The capital cost of

this turbine is taken as \$300,000.00 [56]. The replacement cost is estimated at \$350,000.00, O&M cost is estimated at 2% of the capital cost.

HYDRO 

Name: Abbreviation:

Economics

Capital Cost (\$):	<input type="text" value="300 000.00"/>
Replacement Cost (\$):	<input type="text" value="350 000.00"/>
O&M Cost (\$/yr):	<input type="text" value="6 000.00"/>
Lifetime (years):	<input type="text" value="30.00"/>

Turbine

Available head (m):	<input type="text" value="18.00"/>
Design flow rate (L/s):	<input type="text" value="1 200.00"/>
Minimum flow ratio (%):	<input type="text" value="40.00"/>
Maximum flow ratio (%):	<input type="text" value="100.00"/>
Efficiency (%):	<input type="text" value="85.00"/>

Nominal Capacity: 180.112 kW

Electrical Bus

AC DC

Intake Pipe

Pipe head loss (%):	<input type="text" value="30.00"/>
---------------------	------------------------------------


Systems to consider

Simulate systems with and without the hydro turbine.
 Include the hydro turbine in all simulated systems.

Figure 49: Semonkong hydro power station – 180 kW Francis turbine

3.3.1.6 Diesel generator

The existing diesel generator at Semonkong mini hydro power plant is a SCANIA DA3-AJ550P-5S1 three phase brushless synchronous generator. This model is designed for continuous operation at varying load, with a maximum mean load factor of 70% of rated power over 24 hours of operation. It can handle an accumulated peak overload of 110% for 1 hour in a period of 12 hours. The capital cost is taken as \$300,000.00 [59]. A replacement cost is estimated at \$300,000.00, O&M cost is taken as 2% of the capital cost.

GENERATOR 

Name: Abbreviation:

Properties

Name: **Kohler 410kW Standby**

Capacity: **410 kW**

Fuel: **Diesel**

Fuel curve intercept: 7.65 L/hr

Fuel curve slope: 0.268 L/hr/kW

Emissions

CO (g/L fuel): 12.28

Unburned HC (g/L fuel): 0.72

Particulates (g/L fuel): 0.07

Optimization

Simulate systems with and without this generator
 Include in all systems

Kohler

Electrical Bus

AC DC

Generator Cost

Initial Capital:	<input type="text" value="R300 000,00"/>
Replacement:	<input type="text" value="R300 000,00"/>
O&M (per op. hour):	<input type="text" value="R6,000"/>

Figure 50: Semonkong hydro power station - SCANIA DA3-AJ550P-5S1diesel generator

3.3.1.7 Mini hydro turbine

The existing two water turbines at this site are horizontal axis Francis turbines, unit 1 is rated at 500 kW with a design flow rate of 1.596 m³/s and unit 2 is rated at 1500 kW with a design flow rate of 4.875 m³/s. The system net head is 35.5 m and design flow rate of 6,500 L/s, the capital cost of these turbines is taken as \$500,000.00 [56]. The replacement cost is estimated at \$600,000.00, O&M cost is estimated at 2% of the capital cost.

The screenshot shows the configuration for a 2MW Generic turbine. The interface includes the following sections:

- General:** Name: 2MW Generic, Abbreviation: Hyd1M. Buttons: Remove, Copy To Library.
- Economics:**
 - Capital Cost (\$): 500 000.00
 - Replacement Cost (\$): 600 000.00
 - O&M Cost (\$/yr): 10 000.00
 - Lifetime (years): 30.00
- Electrical Bus:** AC (selected), DC.
- Intake Pipe:** Pipe head loss (%): 15.00
- Turbine:**
 - Available head (m): 35.50
 - Design flow rate (L/s): 6 500.00
 - Minimum flow ratio (%): 20.00
 - Maximum flow ratio (%): 100.00
 - Efficiency (%): 90.00
 - Nominal Capacity: 2,037,292 kW
- Systems to consider:**
 - Simulate systems with and without the hydro turbine.
 - Include the hydro turbine in all simulated systems.

Figure 51: Mantsonyane hydro power station – 2 MW Francis turbine

3.3.1.8 converter

A three-phase bidirectional dual mode hybrid inverter has been selected for this study, this inverter is capable of being used with multiple renewable energy sources in both DC coupling and AC coupling such as solar PV, mini hydro generator and wind turbine generators. The capital cost of the inverter is taken as \$85.00/kW, the replace cost is assumed to be \$75.00/kW with 10% O&M cost.

The screenshot shows the configuration for an Eaton Power Xpert 2250kW inverter. The interface includes the following sections:

- General:** Name: Eaton Power Xpert 2250kW, Abbreviation: Eaton2. Buttons: Remove, Copy To Library.
- Properties:** Name: Eaton Power Xpert 2250kW, Abbreviation: Eaton2250. Includes a download brochure link.
- Costs Table:**

Capacity (kW)	Capital (\$)	Replacement (\$)	O&M (\$/year)
1	\$85.00	\$75.00	\$8.50
- Capacity Optimization:** HOMER Optimizer™ (selected), Search Space. Size (kW) list: 0, 1000, 1500, 2000, 2100, 2200.
- Multiplier:** Three input fields for multiplier values.
- Inverter Input:**
 - Lifetime (years): 15.00
 - Efficiency (%): 98.00
 - Parallel with AC generator?
- Rectifier Input:**
 - Relative Capacity (%): 100.00
 - Efficiency (%): 98.00

Figure 52: Mantsonyane hydro power station – Eaton Xpert 2250 kW

Table 1: Technical Specification of Components

Component	Parameter	Specification	Reference
Canadian Solar MaxPower CS6U- 330P	Nominal Maximum Power (P_{max})	330 W	[60]
	Optimum Operating Voltage (V_{mp})	37.6 V	
	Optimum Operating Current (I_{mp})	9.05 A	
	Open Circuit Voltage (V_{oc})	45.9 V	
	Short Circuit Current (I_{sc})	9.62 A	
	Module efficiency at STC	17.49 %	
	Operating Temperature	-40°C ~ +85°C	
	Nominal Operating Cell Temperature	45±2°C	
	Maximum Fuse Rating	15 A	
	Dimension (mm)	1960 x 992 x 35	
	Life time	25 years	
XANT M-21 Wind Turbine	Rated Power	100 kW	[55]
	Rotor Diameter	21.0 m	
	Hub Height	23, 31, 38	
	Cut in Wind Speed	3.0 m/s	
	Rated Wind Speed	11.0 m/s	
	Cut off Wind Speed	20.0 m/s	
	Survival Wind speed	70 m/s	
	Life time	20 years	
Hydraulic Francis Turbine (Semonkong)	Shaft axis	Horizontal	[61]
	Nominal output	180 KW	
	Rated speed	1500 rpm	
	Rated discharge	1.2 m ³ /s	
	Rated head	18 m	
	Life time	30 years	
SCANIA diesel generator (Semonkong)	Generator Type	Brushless Synchronous	[59]
	Rated voltage	400 V	
	Rated current	526.8 A	
	Number of phases	3	
	Rated power factor	0.8	
	Rated power	400 kW	
	Rated speed	1500 rpm	
	Rated frequency	50 Hz	
	Life time	15 000 hours	
Lithium Ion Battery package	Nominal voltage	600 V	[57]
	Nominal capacity (MWh)	1 MWh	
	Efficiency	90%	
	Life time	15 years	
Bidirectional inverter	Nominal voltage (V_{dc})	600 - 900 V	[58]
	Rated power	500 kW	

Component	Parameter	Specification	Reference
	Max. Charging current	873 A	
	Max. Battery current	900 A	
	Inverter peak efficiency	94%	
	AC output voltage	400V(L-L) 240V(L-N)	
	Output frequency	50/60 Hz	
	Output waveform	Sine wave	
	Max. AC current	720 A	
	Life time	10 years	
Hydraulic Fancis Turbine (Unit 1 Mantsonyane)	Shaft axis	Horizontal	[61]
	Nominal output	500 KW	
	Rated speed	1500 rpm	
	Rated discharge	1.596 m ³ /s	
	Rated head	35.5 m	
	Generator Type	Brushless Synchronous	
	Life time	30 years	
Hydraulic Fancis Turbine (Unit 2 Mantsonyane)	Shaft axis	Horizontal	[61]
	Nominal output	1500 KW	
	Rated speed	1500 rpm	
	Rated discharge	4.875 m ³ /s	
	Rated head	35.5 m	
	Generator Type	Brushless Synchronous	

4 CHAPTER 4: SIMULATION RESULTS AND DISCUSSIONS

This section presents and discusses the economic and technical performance results of all the possible hybrid systems under study. The purpose of introducing renewable energy system to Semonkong mini hydro power plant is to reduce the use of diesel in generation of electricity and to meet the load demand with more renewables. Similarly, the purpose of introducing other sources at Mantsonyane hydropower plant is to ensure a constant generation of 2 MW or more for injection to the grid. Based on the energy resources available and the load demand, HOMER Pro simulates all the possible and feasible system configurations with all of the specified components in the input. The following subsections will be discussing the techno economic feasibility analysis of PV-wind-diesel-battery-hydro system. The HOMER Pro simulation results cover optimization and sensitivity analysis.

4.1 Semonkong Off-Grid Hybrid Power Station

4.1.1 Simulation Results HRES

Based on component sizes, fuel cost, capital cost, input sensitivity parameters as well as assumptions considered in this study, the simulation results produced the following feasible solutions for Semonkong site. This system is comprising of one wind turbine rated at 100 kW, a 410kW diesel generator, a 1MWh storage battery, 180 kW hydro turbine and 500 kW converter. The main selection criteria for optimal system in HOMER is the total Net Present Cost (NPC), as presented in Figure 53. It can be observed that the feasible hybrid system configurations are listed in ascending order of their total NPC. In consideration of NPC and LCOE, it can be seen that PV-wind-diesel-battery-hydro hybrid system is the most cost-effective, reliable and environmentally friendly solution for Semonkong.

The LCOE for Semonkong's option is \$0.129/kWh which is equivalent to M1.75/kWh with Renewable Fraction (RF) of 97.3%. This high percentage of RF indicates that the proposed system operated mainly on renewable energy with a significant reduction in use of fossil fuel. These results are taken at the solar irradiation of 5.44 kWh/m², wind speed of 9.71 m/s, flow rate of 1,595 L/s and the diesel price of \$1.00/L. This project demands an initial capital contribution of roughly \$1.25M with a total NPC of \$2.65M, as illustrated in Figure 53. The findings of this research indicate that integration of renewable energy sources to Semonkong system would cut down diesel

generator operating hours as well as the carbon emissions. In addition to that, the study demonstrates availability of supply to Semonkong community even during dry season.

These findings reflect a similar picture to what Thamae found in his study in 2018 on Semonkong mini hydro power station [39]. His study found the LCOE of a hydro-wind-diesel-battery combination to be US\$0.23/kWh, the resulting renewable energy fraction of 89% as for total annual energy production, wind, hydro and diesel contributed 35%, 54%, and 11% respectively. He concluded that diesel generator backup would continue to be part of the system to ensure reliability and quality of supply in the event that renewables are low for adequate energy production. However, the notable difference between these two studies is that his study did not include solar PV as part of the optimal solution for Semonkong system. This difference could be due to slight differences in resource data used for these two studies.

In a similar study carried out in Benin in 2020 by Odou et al [37], the main findings were also similar to what this study found. The proposed PV-Wind-diesel-battery system was found to be environmentally friendly with only 3% carbon emission and a 96.7% renewable energy penetration. Even though the hydro potential is high at this site, it could not be considered due to remoteness to the village.

	CS6U-330P (kW)	M-21	KohI410 (kW)	1MLI	Hyd100 (kW)	Sinexcel 500 (kW)	Dispatch	COE (\$)	NPC (\$)	Operating cost (\$/yr)	Initial capital (\$)	Ren Frac (%)	Total Fuel (L/yr)
	360	1	410	1	180	500	LF	\$0,129	\$2,65M	\$70 874	\$1,25M	97.3	9 564
		2	410	1	180	500	LF	\$0,153	\$3,14M	\$98 537	\$1,19M	96.4	12 776
	540	2	410		180	500	CC	\$0,159	\$3,26M	\$106 692	\$1,15M	90.1	34 908
	260	2		2	180	500	CC	\$0,170	\$3,49M	\$117 505	\$1,17M	100	0
		4		2	180	500	CC	\$0,218	\$4,49M	\$166 826	\$1,19M	100	0

Figure 53: Semonkong hybrid power system simulation results (LCOE optimized)

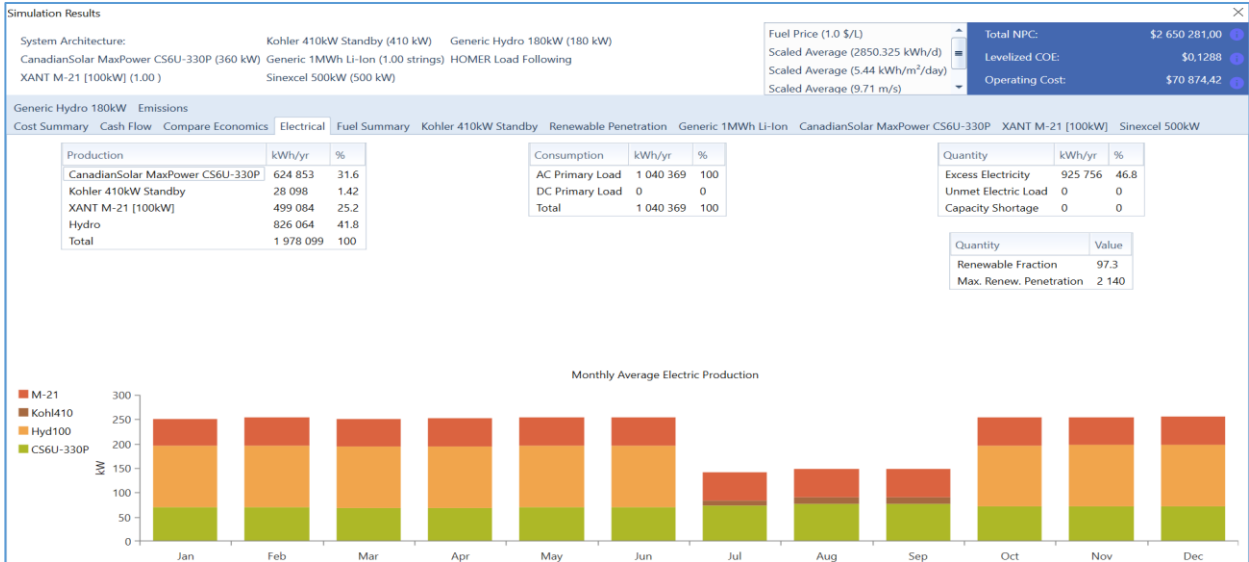


Figure 54: Electricity generation and consumption (LCOE optimized) – Semonkong

CS6U-330P (kW)	M-21	Kohl410 (kW)	1MLI	Hyd100 (kW)	Sinexcel 500 (kW)	Dispatch	COE (\$)	NPC (\$)	Operating cost (\$/yr)	Initial capital (\$)	Ren Frac (%)	Total Fuel (L/yr)
540	2	410		180	500	LF	\$0,159	\$3,26M	\$106 692	\$1,15M	90.1	34 908
	2	410	1	180	500	LF	\$0,153	\$3,14M	\$98 537	\$1,19M	96.4	12 776
360	1	410	1	180	500	LF	\$0,129	\$2,65M	\$70 874	\$1,25M	97.3	9 564
260	2		2	180	500	LF	\$0,170	\$3,49M	\$117 505	\$1,17M	100	0
	4		2	180	500	LF	\$0,218	\$4,49M	\$166 826	\$1,19M	100	0

Figure 55: Semonkong hybrid power system simulation results (RF optimized)

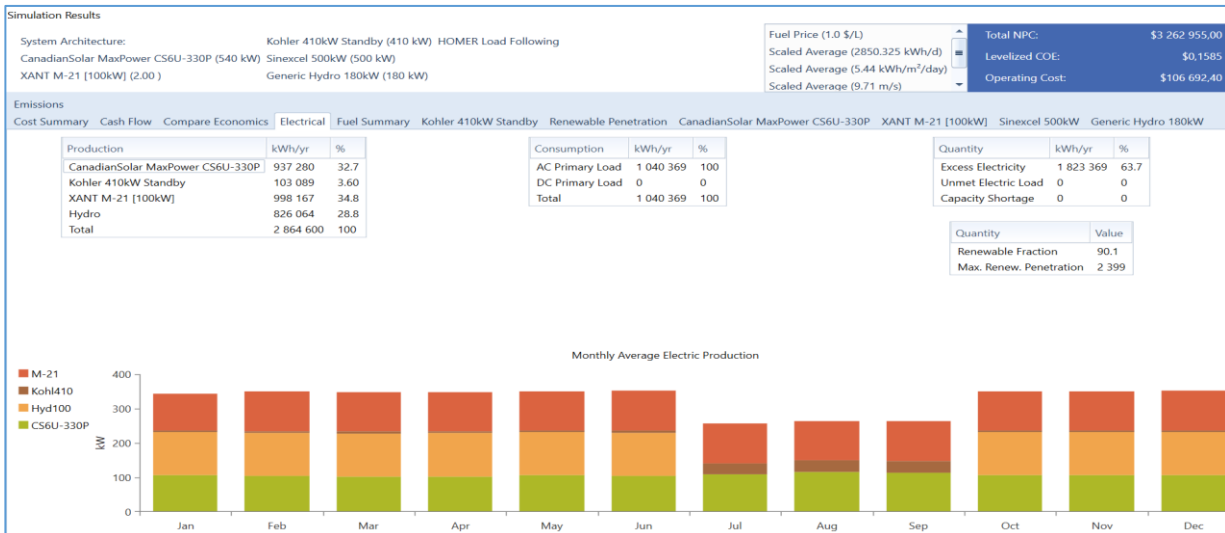


Figure 56: Electricity generation and consumption (RF optimized) – Semonkong

4.1.2 Optimization Results

With reference to simulation results in Figure 53, the system was optimized with LCOE and the most cost-effective combination came out to be solar PV-wind-diesel-battery-hydro. The resulting LCOE for this configuration is \$0.129/kWh while NPC is \$2.65M with the RF of 97.3%. It can be noted that introducing this combination of renewable energy technologies at Semonkong would cut down the costs of diesel and emissions thus enhancing good environmental quality. Hazardous substances which were resulting from diesel fuel emissions would dramatically be cut down.

The total energy produced by this system is 1,978,099 kWh/year. Out of this energy produced, 499,084 kWh is contributed by wind turbine generator and this translates to 25.2% while diesel generator contributed 28,098 kWh which is about 1.42%, solar PV contribution is 624, 853 kWh/year (31.6%) and hydro power generation is 826,064 kWh (41.8%). The primary load of 1,040,369 kWh/year was met with the excess electricity of 925,756 kWh/year which is about 46.8% of the annual energy production. The excess generation can be used to supply any additional load that may be connected as a result of business growth and other upcoming activities around the area. It can be observed that each unit produced different amounts of electricity from month to month. This monthly difference in generation is as a result of variability in monthly mean wind speed, global solar radiation and mean river flow rates. During the wet season, from October up to June, the flow rates are high enough for hydropower plant to contribute a significant amount of electricity to the load.

During this period, the emissions from diesel fuel are zero because the diesel generator never generated power. It can be seen that wind generator consistently produced about 40 kW throughout the year with no production from hydro power plant from July to September. Referring to Figure 57, the average fuel consumption is 26.2 L/day as opposed to the current diesel consumption of 600 L/day at Semonkong generation plant. This reduction in fuel consumption is proportional to a reduction in carbon emissions which translates to about 95.6 %. As a matter of fact, a diesel generator at Semonkong mini hydro was intended to serve as a backup generation to serve the load when the water levels are low for hydro system to meet the demand. But it can be seen that diesel generator serves as the main source of power with the operating factor of about 90% as illustrated in Figure 4.

When optimizing the system with RF in Figure 55, it is noticed that the most cost-effective combination becomes PV-wind-diesel-hydro, this new combination has eliminated energy storage therefore the resulting LCOE for this configuration is \$0.159/kWh while NPC increased by 18.71% from \$2.65M to \$3.26M with the RF drop from 97.3% to 90.1%. As illustrated in Figure 56, the total energy produced by this configuration increased by 31% from 1,978,099 kWh/year to 2,864,600 kWh/year. Out of this energy produced, 998,167 kWh is contributed by wind turbine generator and this translates to 34.8% while diesel generator contributed 103,089 kWh which is about 3.6% and hydro power generation is kept at 826,064 kWh (41.8%). The primary load of 1,040,369 kWh/year was met with the excess electricity of 1,823,369 kWh/year which is about 63.7% of the annual energy production.

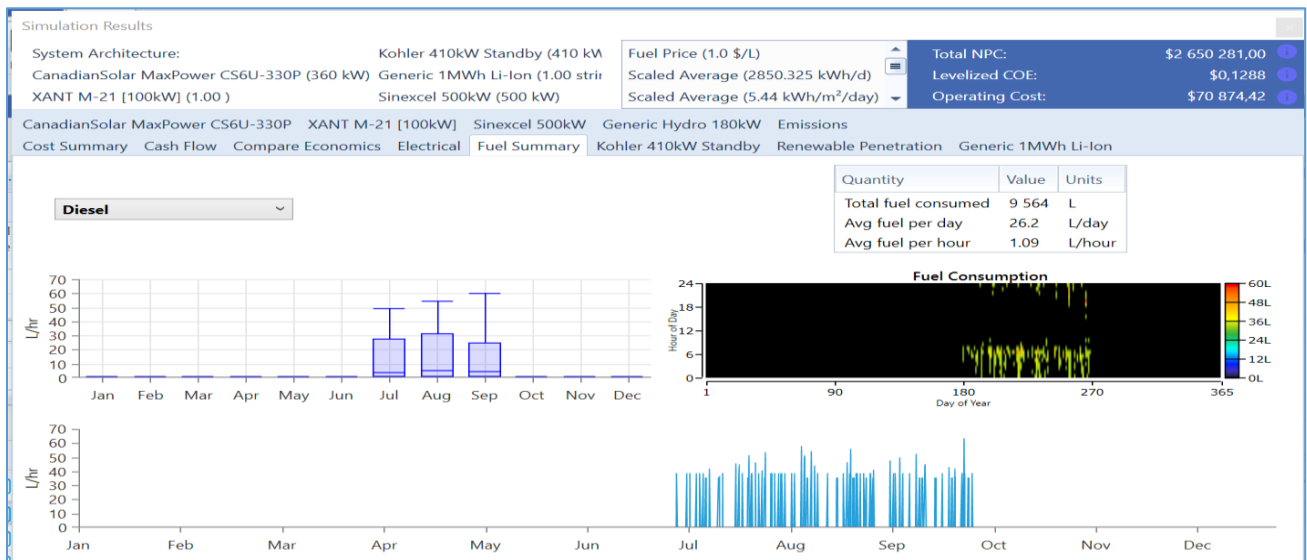


Figure 57: Fuel summary for Semonkong HRES

4.1.3 Sensitivity Analysis Results

In order to check the impact of variation of the following input parameters, wind speed, fuel price, river flow rates, solar radiation primary load, the sensitivity analysis was performed on both systems. This gives the picture of future effects of uncertainties regarding the input parameters over the entire project life. Figure 58 indicates the impact of fuel price and load variation on COE for Semonkong HRES, the O&M is represented by the surface of the chart while the COE is superimposed on the surface. It can be noted that if the primary load increases from 2,300 kWh/d to 3,300 kWh/d at a diesel price of \$1/L and the wind speed fixed at 9.71 m/s, the cost of energy drops from \$0.148/kWh to \$0.121/kWh while the operation and maintenance cost increases from about \$60,400 to around \$62,800. This reveals that a very low load on this plant would results in

a high COE and a comparatively low O&M costs. It is also observed that the operation and maintenance cost is not sensitive to variation in diesel cost. As an example, if the electric load remains at 2,500 kWh/d and the fuel price increases from \$0.5/L to \$1.5/L, the O&M remains at around \$60,800.

Figure 59 shows the effect of river flow rate and discount rate on the COE and NPC for Semonkong HRES. The NPC is represented by the surface of the chart while the COE is superimposed on the surface. It can be observed that as the discount rate increase from 7% to 9.36% when flow rate is kept at 1000 L/s the COE also increases from \$0.121/kWh to \$0.140/kWh while the NPC drops from about \$2,800 000 to \$2,520 000. As a matter of fact, according to this analysis, a high rate of discount results in a high unit price. Considering the impact of variation in flow rate on NPC and COE, it can be seen that variation of river flow rate does not have any impact on the two parameters.

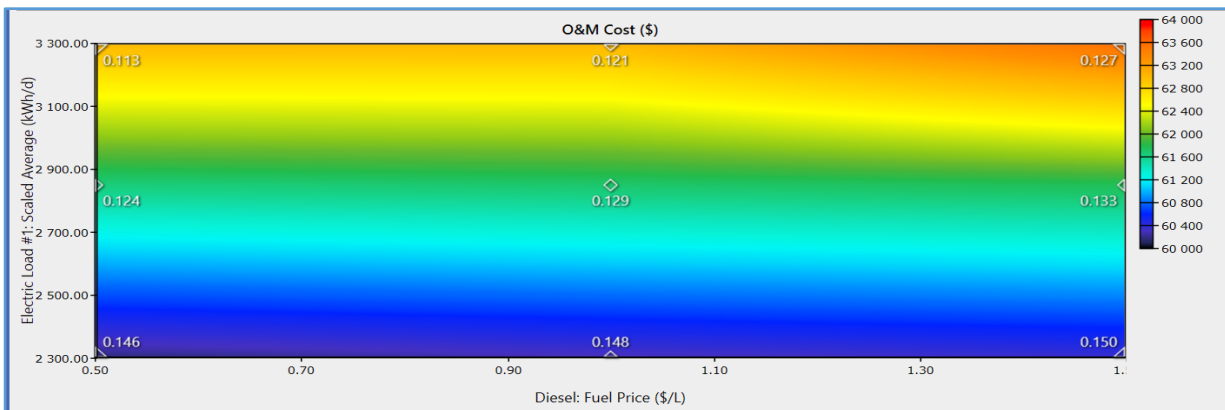


Figure 58 : Effects of fuel price and load variation on the COE and O&M cost – Semonkong HRES

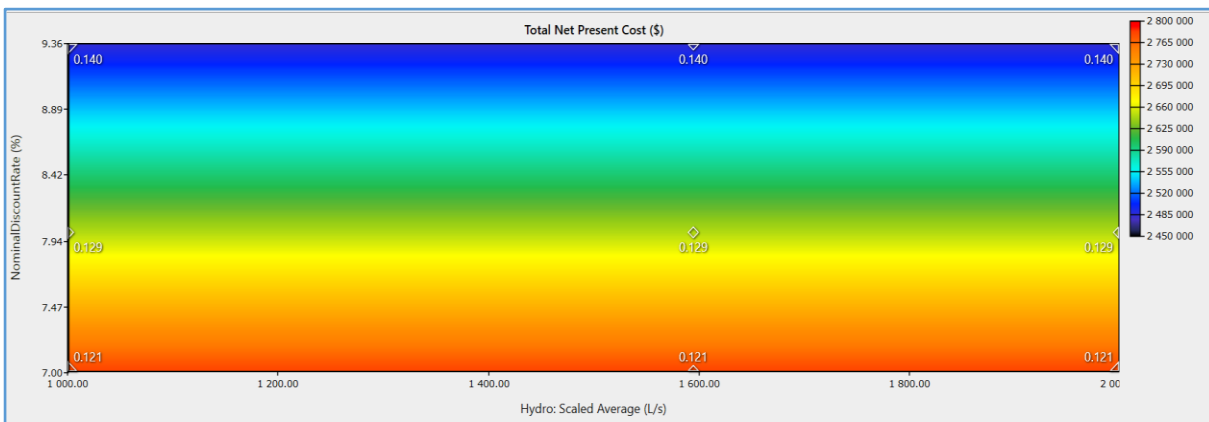


Figure 59: Effect of river flow rate and discount rate on the COE and NPC – Semonkong HRES

4.2.3 Sensitivity Analysis Results

Figure 64 indicates the impact of solar radiation and river flow rate on capacity shortage and COE for Mantsonyane HRES, the chart surface represents the capacity shortage while the COE is superimposed on the surface. It is observed that as the flow rate increases from 1400 L/s to 2000 L/s the COE decreases from \$0.156/kWh to \$0.150/kWh regardless of how much the solar radiation is. The capacity shortage drops from 3,520 kWh/year to 3,220 kWh/year. This implies that the good flow rates would result in a more affordable unit price. The results also show that the variation of solar radiation does not have any impact on COE and the capacity shortage when the discharge rate is less than 1,520 L/s.

The effects of solar radiation and wind speed on COE and AEP is depicted in Figure 65. The AEP is represented by chart surface while the COE is superimposed on the surface of the chart. As the wind speed increases from 6 m/s to 12 m/s, the COE decreases from \$0.176/kWh to \$0.151/kWh while the AEP increased from 15,600,000 kWh to 19,800,000 kWh. This implies that the amount of energy production follows the wind speed, similarly the system unit price becomes even more affordable at higher wind speeds.

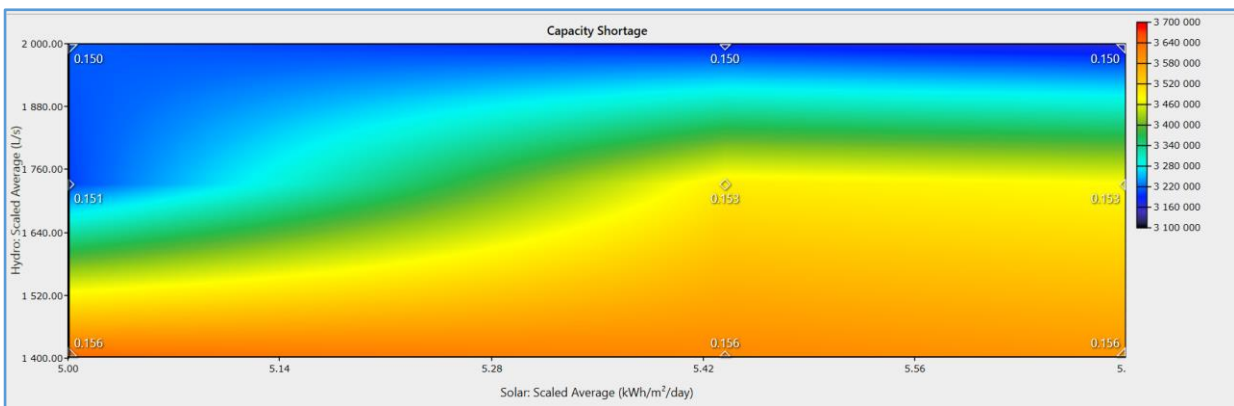


Figure 64: Effects of solar radiation and flow rate on capacity shortage and COE – Mantsonyane HRES

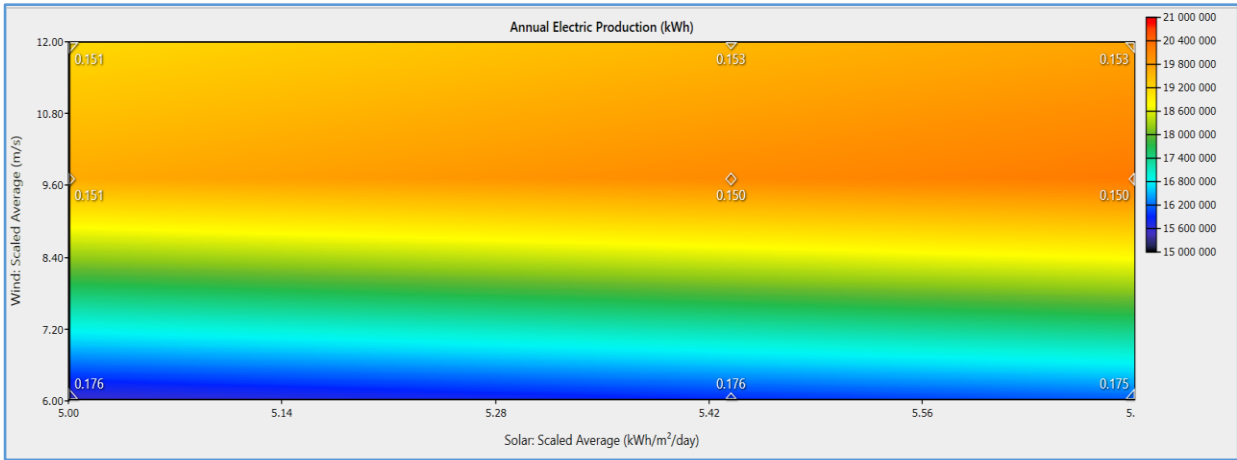


Figure 65: Effects of solar radiation and wind speed on COE and Annual Energy Production – Mantsonyane HRES

5 CHAPTER 5: CONCLUSION AND RECOMMENDATIONS

The aim of this study was to assess the viability of developing a hybrid renewable energy system for a grid connected system at Mantsonyane so that at least 2 MW is injected to the grid all the time. Equally important aim of the study was to reduce diesel consumption and carbon emissions at Semonkong hydro-diesel plant by introduction of renewable energy sources and battery storage. HOMER Pro software was used to perform the analysis of the optimum HRES, while the viability was assessed based on COE, NPC and carbon emissions of the system.

The simulation results indicate that the optimum solution for Semonkong site is a PV-Wind-Diesel-Battery-Hydro hybrid system. This system is made up of 360 kW of solar PV array, 100 kW wind turbine, 500 kW inverter, 1 MWh battery storage, 180 kW mini hydro and 410 kW diesel generator with a load following dispatch strategy. This combination resulted in a COE of \$0.129/kWh, NPC of \$2.65M and the fuel consumption of 26.2 L/day for generator operation for only 3 months in a year. In addition, the annual power generation of this combination is 1,978,099 kWh, of which 31.6 % is contributed by solar PV, diesel generator delivered 1.42% only, wind turbine generator produced 25.2 % and hydro contribution is 41.8 %. Given a high RF of 97.3% for this optimal combination, the diesel consumption is as low as 26.2 L/day which is around 9,564 L in a year since it only operates for 3 months.

Moreover, this system was investigated with the application of sensitivity analysis using the following variables, wind speed, solar radiation, river flow rate, NPC, capacity shortage and annual production. The analysis reveals that a very low load on this plant would results in a high COE and a comparatively low O&M costs. It is also observed that the operation and maintenance cost is not sensitive to variation in diesel cost as illustrated in Figure 58. As an example, if the electric load remains at 2,500 kWh/d and the fuel price increases from \$0.5/L to \$1.5/L, the O&M cost remains at around \$60,800. Considering the impact of variation in flow rate on NPC and COE, it can be seen that variation of river flow rate does not have any impact on the two parameters, this is shown in Figure 59.

As for Mantsonyane study site, it is observed from Figure 64 that when the flow rate increases from 1400 L/s to 2000 L/s the COE decreases from \$0.156/kWh to \$0.150/kWh, this behavior is not influenced by solar radiation at all. The capacity shortage drops from 3,520 kWh/year to 3,220

kWh/year. This implies that the good flow rates would result in a more affordable unit price. The results also show that the variation of solar radiation does not have any impact on COE and the capacity shortage when the discharge rate is less than 1,520 L/s. It is also noted that as the wind speed increases from 6 m/s to 12 m/s, the COE decreases from \$0.176/kWh to \$0.151/kWh while the AEP increased from 15,600,000 kWh to 19,800,000 kWh. This confirms that the amount of energy production follows the wind speed, similarly the system unit price becomes even more affordable at higher wind speeds which makes this project viable at this site since the average wind speed is around 9.71 m/s.

The findings from this study show that Semonkong optimal configuration experience a minimal impact from the instability of input variables like diesel price, river flow rate and solar radiation. The generation results (Figure 63) of Mantsonyane indicates a very low production from a mini hydro as a result of low average river flow rates. It can be confirmed that this system operates at a very low efficiency which makes it expensive to operate, so the intervention of this study was to also improve the system efficiency by adding more renewables to the existing mini hydropower plant.

Due to the absence of solar and wind ground data for Mantsonyane site, data extracted from NASA was used for modelling the system. Therefore, it is also recommended that further similar studies at Mantsonyane site should use actual measured ground data not satellite derived data in order to acquire more definite outcomes of the viability of the HRES.

Reference

- [1] D. Neves, C. A. Silva, and S. Connors, "Design and implementation of hybrid renewable energy systems on micro-communities: A review on case studies," *Renew. Sustain. Energy Rev.*, vol. 31, pp. 935–946, Mar. 2014, doi: 10.1016/j.rser.2013.12.047.
- [2] J. Kartite and M. Cherkaoui, "Study of the different structures of hybrid systems in renewable energies: A review," *Energy Procedia*, vol. 157, pp. 323–330, Jan. 2019, doi: 10.1016/j.egypro.2018.11.197.
- [3] M. Antwi and D. D. Sedegah, "Climate Change and Societal Change—Impact on Hydropower Energy Generation," in *Sustainable Hydropower in West Africa*, Elsevier, 2018, pp. 63–73.
- [4] B. Hamududu and Å. Killingtveit, "Hydropower Production in Future Climate Scenarios; the Case for the Zambezi River," *Energies*, vol. 9, no. 7, p. 502, Jun. 2016, doi: 10.3390/en9070502.
- [5] L. Lesotho Electricity and Water Authority, "LEWA annual_report_17-18.pdf." LEWA, 2018.
- [6] "Welcome to HOMER." <https://www.homerenergy.com/products/pro/docs/latest/index.html> (accessed Oct. 22, 2019).
- [7] G. Falchetta, D. E. H. J. Gernaat, J. Hunt, and S. Sterl, "Hydropower dependency and climate change in sub-Saharan Africa: A nexus framework and evidence-based review," *J. Clean. Prod.*, vol. 231, pp. 1399–1417, Sep. 2019, doi: 10.1016/j.jclepro.2019.05.263.
- [8] K. Deveci and Ö. Güler, "A CMOPSO based multi-objective optimization of renewable energy planning: Case of Turkey," *Renew. Energy*, vol. 155, pp. 578–590, Aug. 2020, doi: 10.1016/j.renene.2020.03.033.
- [9] Y. R. Pasalli and A. B. Rehiara, "Design Planning of Micro-hydro Power Plant in Hink River," *Procedia Environ. Sci.*, vol. 20, pp. 55–63, 2014, doi: 10.1016/j.proenv.2014.03.009.
- [10] S. Sinha and S. S. Chandel, "Review of recent trends in optimization techniques for solar photovoltaic–wind based hybrid energy systems," *Renew. Sustain. Energy Rev.*, vol. 50, pp. 755–769, Oct. 2015, doi: 10.1016/j.rser.2015.05.040.
- [11] R. Mahmood, S. Jia, A. Lv, and W. Zhu, "A preliminary assessment of environmental flow in the three rivers' source region, Qinghai Tibetan Plateau, China and suggestions," *Ecol. Eng.*, vol. 144, p. 105709, Feb. 2020, doi: 10.1016/j.ecoleng.2019.105709.
- [12] M. O. Abdullah, V. C. Yung, M. Anyi, A. K. Othman, K. B. Ab. Hamid, and J. Tarawe, "Review and comparison study of hybrid diesel/solar/hydro/fuel cell energy schemes for a rural ICT Telecenter," *Energy*, vol. 35, no. 2, pp. 639–646, Feb. 2010, doi: 10.1016/j.energy.2009.10.035.
- [13] L. Barelli, L. Liucci, A. Ottaviano, and D. Valigi, "Mini-hydro: A design approach in case of torrential rivers," *Energy*, vol. 58, pp. 695–706, Sep. 2013, doi: 10.1016/j.energy.2013.06.038.
- [14] T. Aukitino, M. G. M. Khan, and M. R. Ahmed, "Wind energy resource assessment for Kiribati with a comparison of different methods of determining Weibull parameters," *Energy Convers. Manag.*, vol. 151, pp. 641–660, Nov. 2017, doi: 10.1016/j.enconman.2017.09.027.
- [15] C. K. Pandey and A. K. Katiyar, "Solar Radiation: Models and Measurement Techniques," *Journal of Energy*, 2013. <https://www.hindawi.com/journals/jen/2013/305207/> (accessed Jan. 13, 2020).
- [16] J. A. Otkin, M. C. Anderson, J. R. Mecikalski, and G. R. Diak, "Validation of GOES-Based Insolation Estimates Using Data from the U.S. Climate Reference Network," *J. Hydrometeorol.*, vol. 6, no. 4, pp. 460–475, Aug. 2005, doi: 10.1175/JHM440.1.
- [17] K. M. Ng, N. M. Adam, O. Inayatullah, and M. Z. A. Ab. Kadir, "Assessment of solar radiation on diversely oriented surfaces and optimum tilts for solar absorbers in Malaysian tropical latitude," *Int. J. Energy Environ. Eng.*, vol. 5, no. 1, p. 75, Mar. 2014, doi: 10.1007/s40095-014-0075-7.
- [18] T. M. Azerefegn, R. Bhandari, and A. V. Ramayya, "Techno-economic analysis of grid-integrated PV/wind systems for electricity reliability enhancement in Ethiopian industrial park," *Sustain. Cities Soc.*, vol. 53, p. 101915, Feb. 2020, doi: 10.1016/j.scs.2019.101915.

- [19] “EREC – EUROPEAN RENEWABLE ENERGY COUNCIL – C-Energy 2020.” <http://www.c-energy2020.eu/eu-networks/erec-european-renewable-energy-council/> (accessed Nov. 04, 2019).
- [20] W. Uddin *et al.*, “Current and future prospects of small hydro power in Pakistan: A survey,” *Energy Strategy Rev.*, vol. 24, pp. 166–177, Apr. 2019, doi: 10.1016/j.esr.2019.03.002.
- [21] J. Chang, X. Wang, Y. Li, Y. Wang, and H. Zhang, “Hydropower plant operation rules optimization response to climate change,” *Energy*, vol. 160, pp. 886–897, Oct. 2018, doi: 10.1016/j.energy.2018.07.066.
- [22] C. S. Kaunda, C. Z. Kimambo, and T. K. Nielsen, “Potential of Small-Scale Hydropower for Electricity Generation in Sub-Saharan Africa,” *ISRN Renew. Energy*, vol. 2012, pp. 1–15, 2012, doi: 10.5402/2012/132606.
- [23] S. J. Williamson, B. H. Stark, and J. D. Booker, “Low Head Pico Hydro Turbine Selection using a Multi-Criteria Analysis,” p. 9.
- [24] M. R. Basir Khan, R. Jidin, J. Pasupuleti, and S. A. Shaaya, “Optimal combination of solar, wind, micro-hydro and diesel systems based on actual seasonal load profiles for a resort island in the South China Sea,” *Energy*, vol. 82, pp. 80–97, Mar. 2015, doi: 10.1016/j.energy.2014.12.072.
- [25] A. H. Elbatran, O. B. Yaakob, Y. M. Ahmed, and H. M. Shabara, “Operation, performance and economic analysis of low head micro-hydropower turbines for rural and remote areas: A review,” *Renew. Sustain. Energy Rev.*, vol. 43, pp. 40–50, Mar. 2015, doi: 10.1016/j.rser.2014.11.045.
- [26] H. Wei, Z. Hongxuan, D. Yu, W. Yiting, D. Ling, and X. Ming, “Short-term optimal operation of hydro-wind-solar hybrid system with improved generative adversarial networks,” *Appl. Energy*, vol. 250, pp. 389–403, Sep. 2019, doi: 10.1016/j.apenergy.2019.04.090.
- [27] Yu. Vorobiev, J. González-Hernández, P. Vorobiev, and L. Bulat, “Thermal-photovoltaic solar hybrid system for efficient solar energy conversion,” *Sol. Energy*, vol. 80, no. 2, pp. 170–176, Feb. 2006, doi: 10.1016/j.solener.2005.04.022.
- [28] Administrator, “Solar Cell I-V Characteristic and the Solar Cell I-V Curve,” *Alternative Energy Tutorials*. <http://www.alternative-energy-tutorials.com/energy-articles/solar-cell-i-v-characteristic.html> (accessed Oct. 13, 2019).
- [29] L. Al-Ghussain, H. Ahmed, and F. Haneef, “Optimization of hybrid PV-wind system: Case study Al-Tafilah cement factory, Jordan,” *Sustain. Energy Technol. Assess.*, vol. 30, pp. 24–36, Dec. 2018, doi: 10.1016/j.seta.2018.08.008.
- [30] S. R. Shah, R. Kumar, K. Raahemifar, and A. S. Fung, “Design, modeling and economic performance of a vertical axis wind turbine,” *Energy Rep.*, vol. 4, pp. 619–623, Nov. 2018, doi: 10.1016/j.egy.2018.09.007.
- [31] A. S. Al Busaidi, H. A. Kazem, A. H. Al-Badi, and M. Farooq Khan, “A review of optimum sizing of hybrid PV–Wind renewable energy systems in oman,” *Renew. Sustain. Energy Rev.*, vol. 53, pp. 185–193, Jan. 2016, doi: 10.1016/j.rser.2015.08.039.
- [32] H. Zhang, Z. Lu, W. Hu, Y. Wang, L. Dong, and J. Zhang, “Coordinated optimal operation of hydro–wind–solar integrated systems,” *Appl. Energy*, vol. 242, pp. 883–896, May 2019, doi: 10.1016/j.apenergy.2019.03.064.
- [33] G. K. K. Reddy, S. V. Reddy, T. K. Ramkumar, and B. Sarojamma, “Wind Power Density Analysis for Micro-Scale Wind Turbines,” p. 9.
- [34] A. Maleki, H. Hafeznia, M. A. Rosen, and F. Pourfayaz, “Optimization of a grid-connected hybrid solar-wind-hydrogen CHP system for residential applications by efficient metaheuristic approaches,” *Appl. Therm. Eng.*, vol. 123, pp. 1263–1277, Aug. 2017, doi: 10.1016/j.applthermaleng.2017.05.100.
- [35] F. H. Mahmood, A. K. Resen, and A. B. Khamees, “Wind characteristic analysis based on Weibull distribution of Al-Salman site, Iraq,” *Energy Rep.*, vol. 6, pp. 79–87, Feb. 2020, doi: 10.1016/j.egy.2019.10.021.

- [36] Z. Liu and L. Zhang, "A review of failure modes, condition monitoring and fault diagnosis methods for large-scale wind turbine bearings," *Measurement*, vol. 149, p. 107002, Jan. 2020, doi: 10.1016/j.measurement.2019.107002.
- [37] O. D. T. Odou, R. Bhandari, and R. Adamou, "Hybrid off-grid renewable power system for sustainable rural electrification in Benin," *Renew. Energy*, vol. 145, pp. 1266–1279, Jan. 2020, doi: 10.1016/j.renene.2019.06.032.
- [38] B. M. Taele, K. K. Gopinathan, and L. Mokhuts'oane, "The potential of renewable energy technologies for rural development in Lesotho," *Renew. Energy*, vol. 32, no. 4, pp. 609–622, Apr. 2007, doi: 10.1016/j.renene.2006.02.014.
- [39] L. Z. Thamae, "Simulation and Optimization of Renewable Energy Hybrid Power System for Semonkong, Lesotho," in *Africa-EU Renewable Energy Research and Innovation Symposium 2018 (RERIS 2018)*, M. Mpholo, D. Steuerwald, and T. Kukeera, Eds. Cham: Springer International Publishing, 2018, pp. 105–115.
- [40] S. Khisa, R. Ebihara, and T. Dei, "Dynamics of a Grid Connected Hybrid Wind-Solar and Battery System: Case Study in Naivasha-Kenya," *Energy Procedia*, vol. 138, pp. 680–685, Oct. 2017, doi: 10.1016/j.egypro.2017.10.200.
- [41] B. Bhandari, K.-T. Lee, C. S. Lee, C.-K. Song, R. K. Maskey, and S.-H. Ahn, "A novel off-grid hybrid power system comprised of solar photovoltaic, wind, and hydro energy sources," *Appl. Energy*, vol. 133, pp. 236–242, Nov. 2014, doi: 10.1016/j.apenergy.2014.07.033.
- [42] "Welcome to HOMER." Accessed: Oct. 22, 2019. [Online]. Available: <https://www.homerenergy.com/products/pro/docs/latest/index.html>.
- [43] A. S. Aziz, M. F. N. Tajuddin, M. R. Adzman, A. Azmi, and M. A. M. Ramli, "Optimization and sensitivity analysis of standalone hybrid energy systems for rural electrification: A case study of Iraq," *Renew. Energy*, vol. 138, pp. 775–792, Aug. 2019, doi: 10.1016/j.renene.2019.02.004.
- [44] A. S. Aziz, "Techno-economic analysis using different types of hybrid energy generation for desert safari camps in UAE," p. 14.
- [45] P. Iemsomboon, T. Pati, and K. Bhumkittipich, "Performance Study of Micro Hydro Turbine and PV for Electricity Generator, Case Study: Bunnasopit School, Nan Province, Thailand," *Energy Procedia*, vol. 34, pp. 235–242, 2013, doi: 10.1016/j.egypro.2013.06.752.
- [46] S. Mandal, B. K. Das, and N. Hoque, "Optimum sizing of a stand-alone hybrid energy system for rural electrification in Bangladesh," *J. Clean. Prod.*, vol. 200, pp. 12–27, Nov. 2018, doi: 10.1016/j.jclepro.2018.07.257.
- [47] A. Coester, M. W. Hofkes, and E. Papyrakis, "Economic analysis of batteries: Impact on security of electricity supply and renewable energy expansion in Germany," *Appl. Energy*, vol. 275, p. 115364, Oct. 2020, doi: 10.1016/j.apenergy.2020.115364.
- [48] Y. Wang, M. Zhao, J. Chang, X. Wang, and Y. Tian, "Study on the combined operation of a hydro-thermal-wind hybrid power system based on hydro-wind power compensating principles," *Energy Convers. Manag.*, vol. 194, pp. 94–111, Aug. 2019, doi: 10.1016/j.enconman.2019.04.040.
- [49] B. Bhandari, K.-T. Lee, G.-Y. Lee, Y.-M. Cho, and S.-H. Ahn, "Optimization of Hybrid Renewable Energy Power Systems: A Review," *Int. J. Precis. Eng. Manuf.-Green Technol.*, vol. 2, pp. 99–112, Jan. 2015, doi: 10.1007/s40684-015-0013-z.
- [50] A. B. Kanase-Patil, R. P. Saini, and M. P. Sharma, "Integrated renewable energy systems for off grid rural electrification of remote area," *Renew. Energy*, vol. 35, no. 6, pp. 1342–1349, Jun. 2010, doi: 10.1016/j.renene.2009.10.005.
- [51] John W. Creswell, *Research Design Qualitative, Quantitative, and Mixed Methods Approaches 3rd edition.pdf (PDFDrive.com).pdf*, Third Edition. India: SAGE, 2009.
- [52] C. R. Kothari, *Research Methodology: Methods and Techniques*. New Age International, 2004.

- [53] A. H. Al-Badi and H. Bourdoucen, "Feasibility analysis of renewable hybrid energy supply options for Masirah Island," *Int. J. Sustain. Eng.*, vol. 5, no. 3, pp. 244–251, Sep. 2012, doi: 10.1080/19397038.2011.610009.
- [54] "Made-in-China.com - Manufacturers, Suppliers & Products in China." <https://www.made-in-china.com/> (accessed Dec. 27, 2019).
- [55] "XANT XANT M-21 - 100,00 kW - Wind turbine." <https://en.wind-turbine-models.com/turbines/1455-xant-xant-m-21> (accessed Dec. 30, 2019).
- [56] "Find quality Manufacturers, Suppliers, Exporters, Importers, Buyers, Wholesalers, Products and Trade Leads from our award-winning International Trade Site. Import & Export on alibaba.com," *Alibaba*. <https://www.alibaba.com> (accessed Dec. 30, 2019).
- [57] K. Mongird *et al.*, "Energy Storage Technology and Cost Characterization Report," PNNL-28866, 1573487, Jul. 2019. doi: 10.2172/1573487.
- [58] "Leonics MTP inverter," Aug. 02, 2020. <http://www.leonics.com/product/renewable/inverter/dl/MTP-410-091.pdf> (accessed Feb. 08, 2020).
- [59] "A J Power AJP550 - Yellogen Ltd." <http://www.yellogen.com/a-j-power-ajp550/487> (accessed Feb. 08, 2020).
- [60] C. S. Inc, "Robben Island Solar System Sheds Light on Legacy of Nelson Mandela," *canadiansolar.com*. <https://www.canadiansolar.com/making-the-difference.html> (accessed Dec. 27, 2019).
- [61] "Table 1 . Specifications for Francis-turbine generator.," *ResearchGate*. https://www.researchgate.net/figure/Specifications-for-Francis-turbine-generator_tbl1_321164098 (accessed Feb. 08, 2020).